Università degli Studi di Trieste
Facoltá di Ingegneria
Corso di Laurea Magistrale in Ingegneria Navale

On the Design of a Deep Sea Surface Mooring

Aracri Simona

Relatore: Prof. Giorgio Contento

1

Contents

Abstract

Con questa tesi si vogliono combinare i caratteri tecnici e teorici del progetto di un ancoraggio di superficie in acque profonde. Sin da subito questo argomento appare difficile ed affascinante: come una nave, la boa di superficie deve "vivere" tra due fluidi differenti e deve affrontare forze dovute alla massa d'acqua sotto la superficie , al vento, alle onde di superficie tra i due fluidi e a fattori ambientali che possono variare con il periodo dell'anno, posizione geografica e condizioni climatico-ambientali. Queste forze non sono costanti nè facili da prevedere, per tanto non sono ancora state modellate perfettamente in matematica. Inoltre la boa stessa ha a che fare con le forze trasmessele dal cavo sotto di essa. Ad oggi non c'è una procedura standard per agevolare questo tipo di progetto, ad ogni modo sono stati scritti diversi programmi per guidare il progettista. Alcuni di essi sono immediati ed offrono un ampia gamma di opzioni progettuali, come l'applicazione di Matlab "Mooring & Design Dynamics" (MDD) scritta da Dewey [1], che però non tratta il problema da un punto di vista dinamico. A causa del fallimento di vari ancoraggi, l'analisi dinamica ha assunto un'importanza sempre maggiore. Tale analisi si è resa realizzabile con lo sviluppo di nuovi programmi e lo studio di precedenti progetti. Quest'ultimo rimane un'importante fonte di apprendimento e miglioramento. L'obiettivo del progetto è sviluppare un ancoraggio, affrontandolo da differenti prospettive e, quindi, con mezzi distinti, paragonandoli alla fine.

Abstract

This work is meant to combine the technical and the abstract features of a deep sea surface mooring design. Right from the start this topic appears to be difficult and charming: as a ship, the surface mooring has to "live" between two different fluids and has to withstand the forces due to the mass of water under the surface, due to the wind, due to waves at the interface of the two fluids and due to environmental factors that can vary with the period of year, location, regional climate and weather factors. These forces are not constant nor easily foreseeable, therefore they are not perfectly modelled in mathematics. Moreover the buoy itself also has to deal with the force of the cable under it. At this moment there is not a standard procedure to facilitate this kind of design, but still several programs have been written to guide the designer. Some of them are immediate and offer a wide range of design options, like the Matlab application Mooring & Design Dynamics (MDD) by Dewey [1], but do not treat the problem from a dynamical point of view. Due to the failure of several moorings, the dynamical analysis has become more and more important and it is now feasible with the development of new programs and with the study of the previous designs. The latter remain an important source of learning and improvement. The aim of the design is to develop a mooring facing it from different points of view and therefore with different means, comparing them in the end.

1 Introduction

The need to collect as much data as possible along the water column about currents, temperature, chemistry of the water, etc., in order to be able to study, to monitor and to model the ocean, made the scientists' interest toward the surface and subsurface mooring design grow. A deep sea surface mooring is a unique structure: it links the surface and the bottom of the sea, up to a depth of 5 km. It is intended to collect data contemporary from the sea and from the atmosphere.

NIOZ wants to deploy a deep sea surface mooring in the North Atlantic Ocean, more precisely at 14 North and 40 West. The Marine Geology Department (GEO) is interested in collecting Sahara dust blown and drifted in that zone.

In order to formulate the design criteria for a deep sea surface mooring, some theoretical and practical suggestions have been considered. Below we discuss several theories on the dynamics of moorings, such as the Lumped Mass Method (LMM) [2], spectral analysis [3] and Boundary Value Problem (BVP) [4]. We also consider some designs such as taut, inverse catenary and hybrid (Sec. 3.1). We describe the logic of the choice of a certain kind of design, taking into account the environmental conditions and the requirement of the mooring. Further on, in Sec. 4 and 5, some computer programs that deal with this kind of design have been described.

2   A mooring for the Sahara dust

The particular mooring that we are interested in, as we said before, has to be designed for the North Atlantic, for 14N and 40W (see Fig. 1).
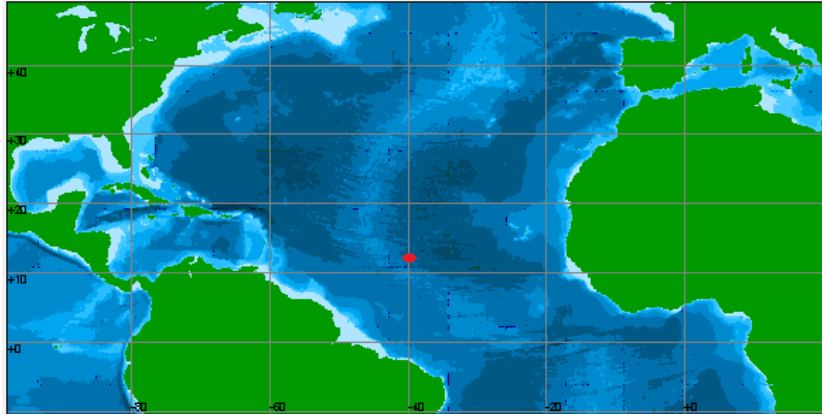

Figure 1: In the figure the red point indicates the mooring desired position [5].

Its main role will be to collect the Sahara dust blown by the wind and carried by the currents until that point. In this spot of the ocean the depth is 5000 m. The principal devices of the mooring are two sediment traps: at 1200 meters of depth and the other at 3500 m, plus a third one on the surface buoy.

The goal of this work is to recommend:

- Design option

- Mooring layout

- Best program to compute both statical and dynamical aspects

As far as the sediment traps and the surface buoy are concerned the GEO department already had suggestions and we are going to maintain their choice (see Sec. 2.1 and 2.2).
Investigating the approach of various institutions, see Table (1) and considering the materials available we can start outlining the mooring.

Reference Person	Institute	Department
Jeffrey Lord Operations Group Leader, Senior Engineering Assistant II	WHOI	Physical Oceanography
Richard P. Trask Research Specialist, Manager, Mooring & Rigging Shop	WHOI	Physical Oceanography
Dr.Gkritzalis-Papadopoulos Sensors Engineer	NOC	Geochemistry Staff
Dr.R.Venkatesan Scientist & Programme Director Ocean Observation Systems	NIOT	Ocean Observation Systems (Program)
Stagg Alastair Regional Manager	Fugro, GEOS	Metocean Measurements
Loic Dussud Head Mechanical Developments	Ifremer	Service Dèveloppements de Systèmes Mècaniques Instrumentaux
Dr.Gerrit Meinecke Project leader marine technology	Marum	Marine Technolgy
Fredrik Dessen Technical Manager	OCEANOR	Fugro OCEANOR
Gert Rohardt Climate Sciences	AWI	Observational Oceanography

Table 1: List of contacts and institutes that work with moorings and gave advise for this project

2.1 Buoy

The Marine Geology department of NIOZ is collaborating with Marum [6], who suggested to use the Dolan buoy, since they previously used it (see Fig. 2 and 3). For this mooring there is the possibility to develop a design for a buoy made ad hoc to hold a dust collector on top, but always starting from the Dolan, therefore in this work we will use the existing buoy.

Buoy characteristics:

- weight: 1.5 tons

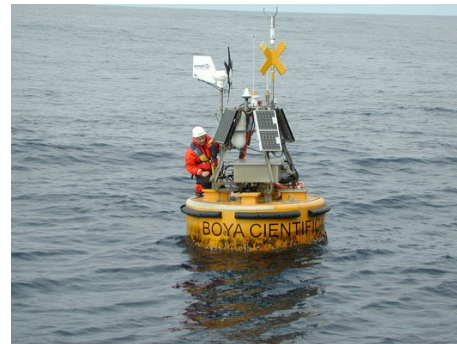- diameter: 2.4 m

Figure 2: Dolan buoy from Marum [7].

Figure 3: Dolan buoy from Marum [8].

2.2 Sediment traps

The sediment traps that are going to be used are made by Technicap, the chosen model, always suggested by the GEO department, is PPS 6/2 (see Fig. 4;5;6). In the vicinity of the sediments traps we also need current meters (Aanderaa).
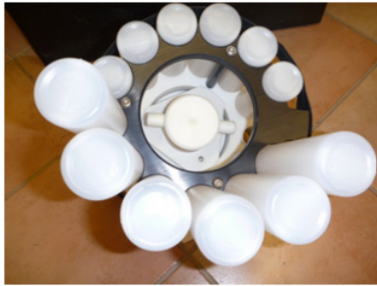

Figure 4: Sediment traps [9]

Figure 5: Sediment Traps [9]

MODEL	PPS 5/2
	1
Shape	Conical (36°)
Baffle material	Phenolic Composite
Baffle Cell diameter	8mm
Aspect ratio of a cell	6,25
Number of Samples	24
Volume of Sampling Bottles *	250ml or 500ml (on request)
Sampling Interval	1 hour - 60 days
Max continuous deployment	18 months
Operating Deph	6000m
MATERIALS	
Trap body	Glass reinforced polyester (GRP) on an alimentary gel-coat
Caroussel	PETP (very hard thermoplastic)
Sampling bottles*	Polypropylen
Electronics / motor pressure case	Titanium GR2 (T40)
Mooring Bar	Titanium GR5 (T6AV)
Power Supply	12 volt AA alkaline batteries pack
Drive motor torque	60kg/cm
Time to shift a bottle	7 seconds
Communications	USB Connector with special programm for XP and VISTA
DIMENSIONS (mm)	
Height	2300
Diameter Max	1330
WEIGHT (kg)	
In Air	110
In Water	45

Figure 6: The figure shows the technical specifications of the sediment traps, such as the chosen model, the used materials, the main dimensions and the weight. [9]

2.3 Programs

As far as the program choice is concerned the main ones used are:

- CABLE by Mark Grosenbaugh (WHOI [10] –NOC [11] –NIOT [12])

- Orcaflex (GEOS [13] –Ifremer [14])

- Deeplines (Ifremer)

- MDD (NIOZ [15])

WHOI's option is the most used and seems to be the best choice regarding the dynamical aspects, therefore for the dynamics **Cable** is the choice. Still it is not really user friendly so is not made for beginners. The **MDD** by Dewey [1], apart to being user friendly, is perfect for the beginners in the field, because, offering immediately a wide choice of wires, chains, buoys, instruments and therefore mooring solutions, allows the designers to gain confidence with their specifications. For all these reasons the first approach with the design will be through MDD. To make clear the physics of the dynamics of the problem, the theoretical approach of the Boundary Value Problem, further discussed below (Sec. 3.4), has been used.

3 Basics

Here we present an overview of previous mooring designs and theories that have been used to compute the dynamic behaviour of a surface mooring. Specifically we present some design options (see Sec. 3.1), we discuss the Lumped Mass Method (see Sec. 3.2), the spectrum analysis (see Sec. 3.3) and the Boundary Value Problem (see Sec. 3.4).

3.1 Design Options

There are two big categories of moorings: subsurface and surface. Differently from the former the surface moorings have to deal with wave forces and with wind, moreover, having a floating buoy it is necessary to prevent this to sink because of these forces. The buoy also needs the possibility to follow the shape of the surface that is changing every moment. Stretchable materials, that are synthetic materials, are used for give to the mooring some "compliance" (ability to stretch) to compensate the large vertical excursions that the buoy may experience during the change of tides and with passing waves and swell. The compliance also compensates the lateral displacement of the buoy on the surface by the drag forces associated with ocean currents. A challenge in the design process, particularly in shallow water, is to achieve an appropriate mix of compliant materials and fish bite-resistant materials, which tend to be unstretchable. One design factor is the "scope" of the mooring, that is the ratio of the total unstretched length of the mooring components to the water depth. A mooring with a scope of less than 1.0 relies on the stretch of the nylon for the anchor to reach the bottom. Such a **taut** mooring remains fairly vertical with a relatively small watch circle[1], but it has a disadvantage: such a vertical mooring is under considerable tension [2], or preloaded, at the time of deployment. Currents and waves impose additional loads beyond the initial preloaded condition. Moorings with scopes between 1.0 and approximately 1.1 are generally referred to as **semitaut** designs [16], (See Fig. 7).

A dynamic study of the behaviour of the mooring showed that the semitaut solution could have a resonant response to the forcing in the range of the wave period, for this reason another option has been proposed: the **inverse catenary** solution. (See Fig. 8). With a typical scope of 1.2. It has wire rope in the upper part then, going down, nylon rope spliced to polypropylene.

The inverse catenary design, offering a larger scope, performs well in high-current periods and still performs well in weak currents. In weak currents, the buoyancy provided by the polypropylene keeps the slightly negatively buoyant nylon from tangling with the rest of the mooring below it. Thus, the inverse catenary design can tolerate a wider range of environmental conditions.
With both the semitaut and the inverse catenary surface mooring designs, it is difficult to make deep-current measurements because the mooring line at these depths is sometimes inclined more than 15 deg from vertical. This is a problem

---

[1]**Watch Circle**
This is the maximum diameter of the circle that can be described by the buoy on the surface of the sea while it remains anchored at the bottom of the ocean.

[2]As we learned studying the MDD application, it is conventional to express the tension at a certain part of the mooring in kg, which is the force at that point divided by the acceleration of gravity g at sea level ($g = 9.81 m/s^2$).
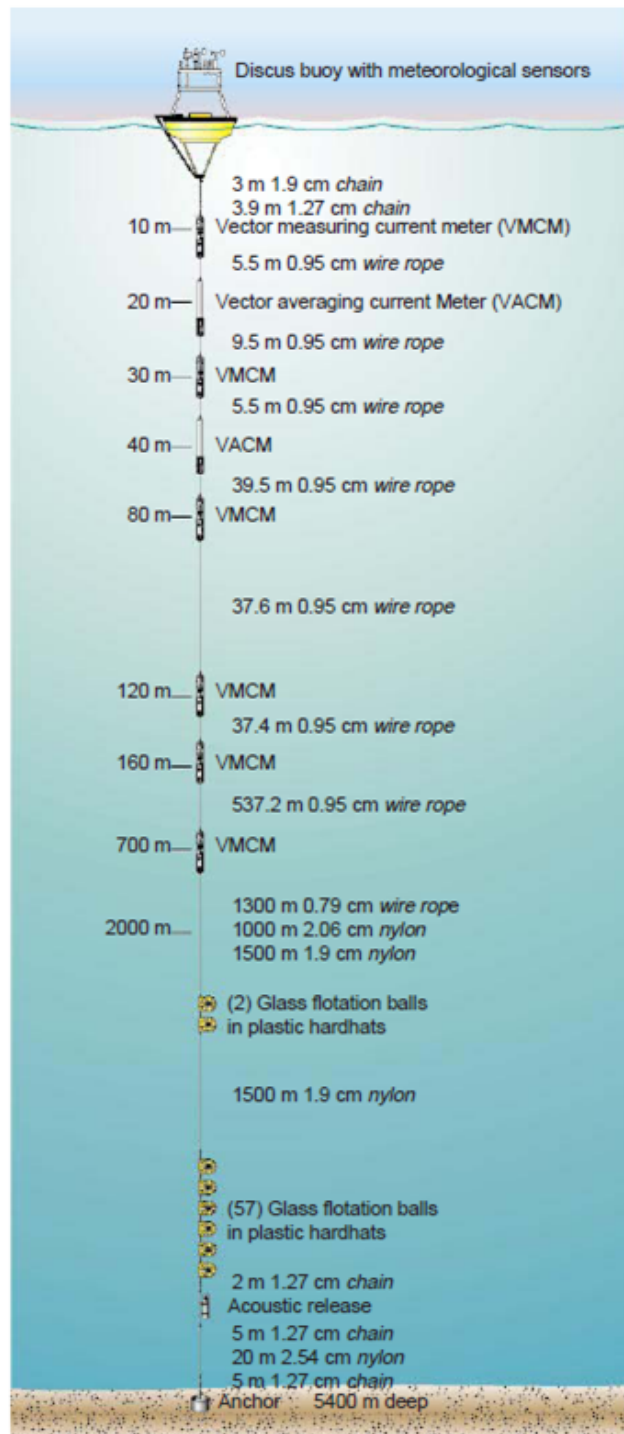
Figure 7: A semitaut surface mooring design. (Design by P.Clay [16])

for two reasons: first, some instruments fitted with compasses do not work well if the compass is inclined more than 15 deg; and second, some velocity sensors require the instrument to be nearly vertical. An inverse catenary mooring, with its greater scope, has inclination problems at shallower depths than the semitaut design. A comparison of the shape of a semitaut design with that of an inverse catenary design when subjected to the same ocean current forcing can be seen in Fig. 9. Note the differences in the horizontal excursions at the surface.

In some regions of the world's oceans, the environmental conditions can be so severe that the instruments attached to the mooring or the mooring itself can fail due to fatigue stresses. In this cases, apart from the choice of an appropriate mooring design, some preventive measure can be taken like **shot peening** [3] some instruments, or by choosing, where possible, different instruments that are less susceptible to fatigue (Fig. 10).

In addition to the inclination problem, there is also a depth-variability problem. Compliant parts of a surface mooring are usually synthetics and must be placed below the fish bite zone. The deep instruments are, therefore, in line in the synthetics; and their depth can vary by several hundred meters depending on the stretch of the material. A pressure sensor on the instrument can be used to record the instrument depth; but if a particular depth is desired, it is not possible with the conventional design. Hence, the trade-off for being able to withstand a wider range of environmental conditions is a reduction in the depth range for making certain kinds of measurements. A partial solution to the problem of deep measurements on a surface mooring is in the mooring design that combines features of both the subsurface and inverse catenary type moorings: **hybrid** (see Fig. 11 and 12). The upper part of the mooring, up to the euphotic zone is similar to any surface mooring, with the instrumentation at the appropriate depths and wire rope in between. The lower part of the mooring from the bottom up to the depth of the instrument is all wire with a cluster of glass ball flotation just above the release near the anchor and one immediately above the instrument. The compliance of the mooring consists of nylon and polypropylene inserted between the deep instrument and the base of the wire at the end of the euphotic zone.

---

[3]**Shot peening** Is a process whereby a component is blasted with small spherical media, called shot, in a manner similar to the process of sand blasting. The medium used in shot peening is more rounded rather than angular and sharp, as in sand blasting. Each piece of shot acts like a small ball-peen hammer and tends to dimple the surface that it strikes. Below the surface, the material tries to restore its original shape, thereby producing below the dimple, a hemisphere of cold-worked material highly stressed in compression. Since cracks usually start at the surface when this is in tension and not in compression, a shot-peened component will take longer to develop a crack, thereby increasing the fatigue life of the part.
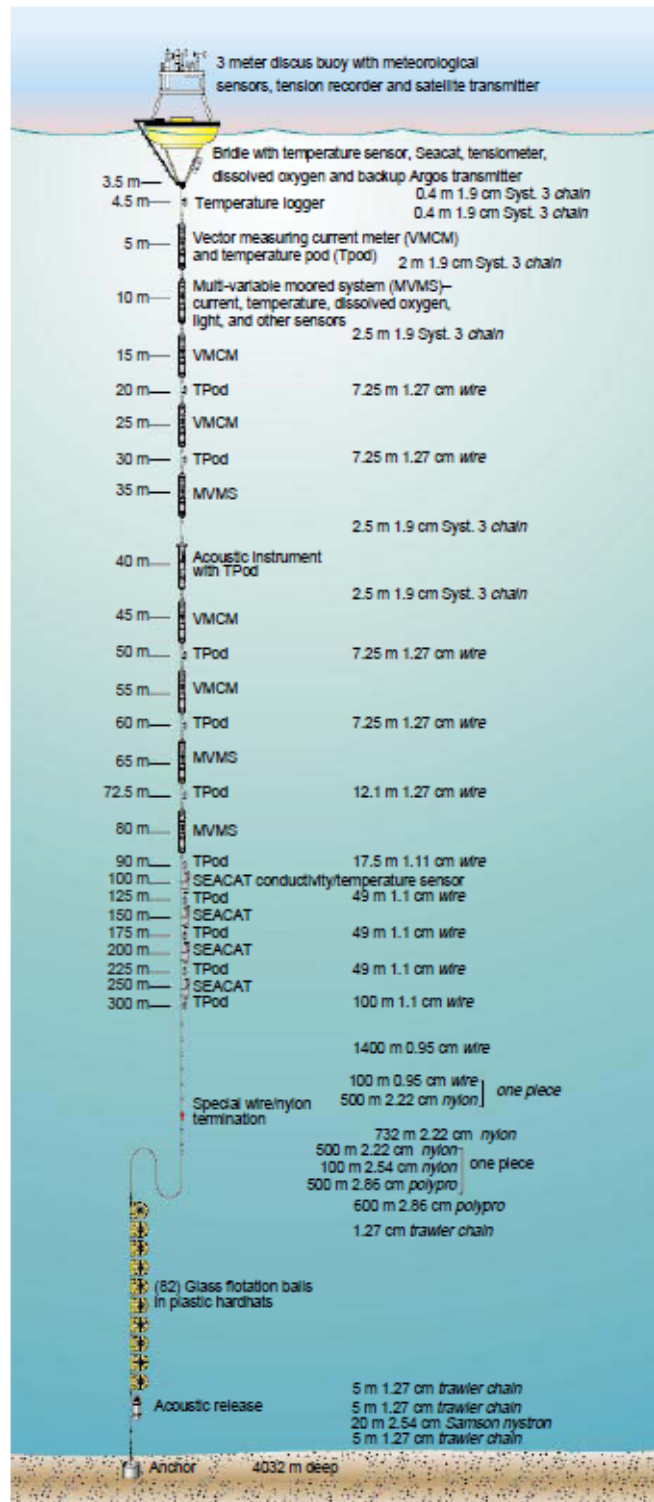
Figure 8: An inverse catenary mooring design. (Design by G.Tupper [16])
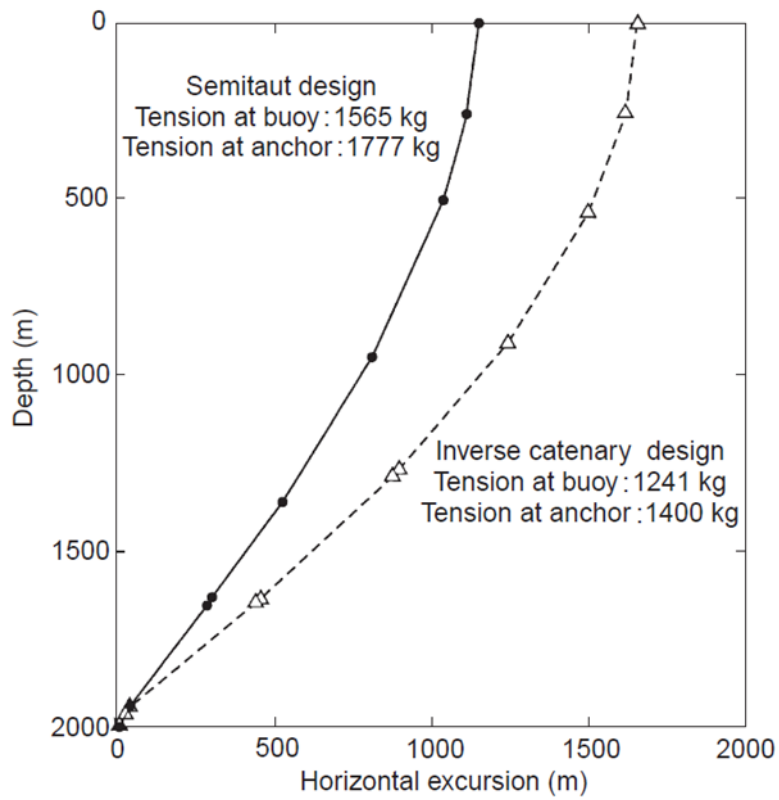
15

Figure 9: Comparison between the horizontal excursion of a semitaut and of an inverse catenary mooring. Vertical axis represents the depth of the water and the horizontal represents the horizontal excursion. The inverse catenary solution allows a bigger horizontal displacements therefore the tensions at the anchor and at the buoy are lower in comparison with the tensions in the semitaut configuration [16].
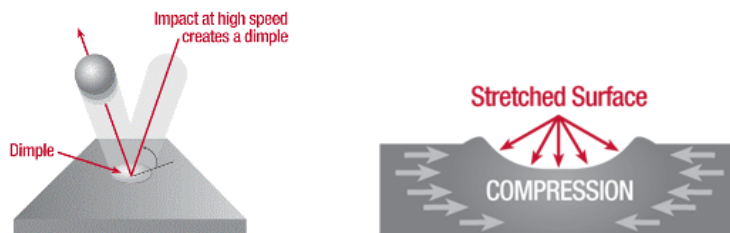

Figure 10: Shot Peening: induced compression on the surface to prevent the crack [17].

16

3 meter discus buoy with meteorological sensors and satellite telemetry

Bridle with T-pod, IMET and VAWR temperature sensors, and tensiometer
6.7 m 1.9 cm *chain*

10 m— Vector measuring current meter (VMCM)

17 m 0.95 cm *wire*

30 m— VMCM

17 m 0.95 cm *wire*

50 m— VMCM

17 m 0.95 cm *wire*

70 m— VMCM

17 m 0.95 cm *wire*

90 m— VMCM

17 m 0.95 cm *wire*

110 m— VMCM

37.3 m 0.95 cm *wire*

150 m— VMCM

47.3 m 0.95 cm *wire*

200 m— VMCM

97 m 0.95 cm *wire*

300 m— VMCM

7.3 m 0.95 cm *wire*

310 m— VMCM

200 m 0.95 cm *wire*
237 m 0.79 cm *wire*

750 m— VMCM

500 m 0.79 cm *wire*
252 m 0.79 cm *wire*

1500 m— VMCM   400 m 0.79 cm *wire*
100 m 0.79 cm *wire*] *one piece*
50 m 2.06 cm *nylon*]
Special wire/nylon termination
450 m *nylon*] *one piece*
500 m 2.54 cm *polypro*]
1.27 cm *trawler chain*
(47) Glass flotation balls
Tensiometer with safety chain
10 m 0.95 cm *wire*

3500 m— VMCM

2078 m 0.95 cm *wire*

1.27 *trawler chain*
(52) Glass flotation balls
1.27 cm *trawler chain*
Acoustic release
5 m 1.27 cm *trawler chain*
20 m 2.54 cm *nylon*
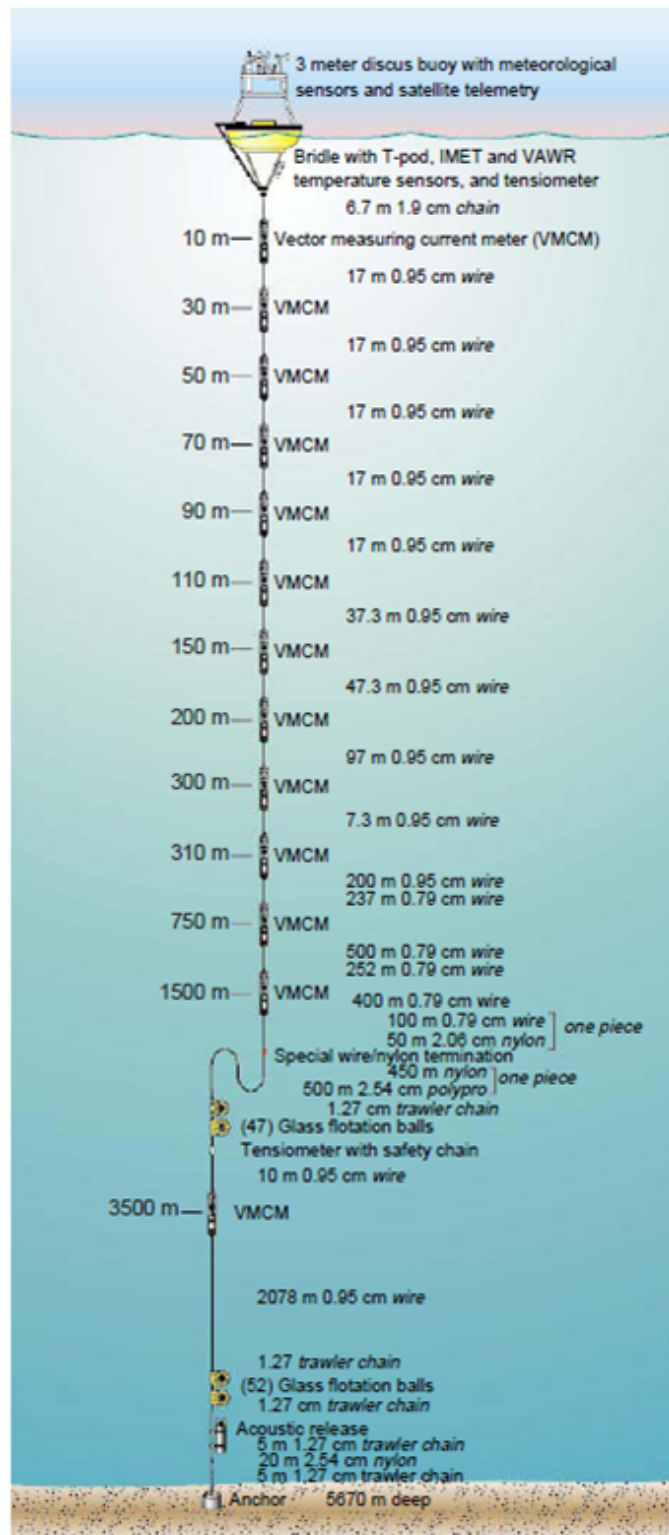5 m 1.27 cm trawler chain
Anchor   5670 m deep

17

Figure 11: Hybrid solution for deep measurement. It has compliant materials just in the middle zone of the mooring, that is typically from the depth of the instruments for deep measurements (in the figure from 3500 m where a VMCM-Vector measuring current meter- is positioned) up to 2000 m depth where the euphotic zone begins. The axes represent the depth and the horizontal excursion. (Design by G.Tupper [16])
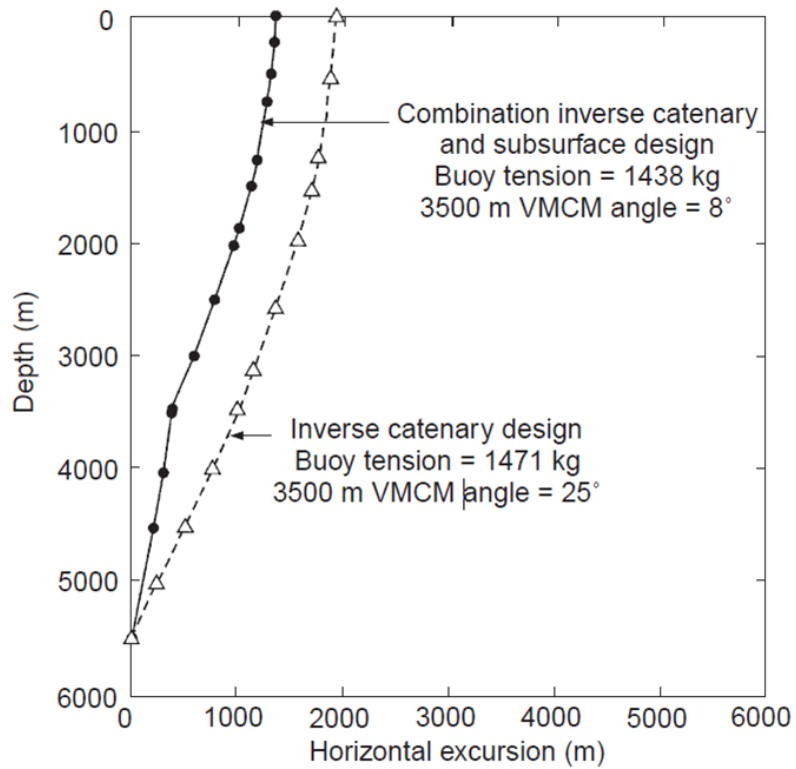
Figure 12: In the figure the vertical axis represents the depth of the water and the horizontal axis represents the horizontal excursion. Here is shown the comparison between a "traditional" inverse catenary mooring and a hybrid solution mooring. The inverse catenary design allows a bigger tilt angle in the bottom part of the mooring where the deep instruments are suppose to be attached, while the hybrid solution behaves better both regarding tilting and buoy tension [16].

18

3.2   Lumped Mass Method

Here we pinpoint the main concepts (italics) for this work from the paper by H. van den Boom [2].

First we describe briefly the two successful discrete elements techniques **The Lumped Mass Method (LMM)** and the **Finite Element Method (FEM)**.

The Lumped Mass Method

The LMM is a computer algorithm set developed to gain further insight in the mechanism of the dynamic behaviour of mooring lines and to quantify the effects of important parameters, with special attention to the maximum tension. The behaviour of a continuous line is modelled as a set of concentrated masses connected by massless springs (see Fig. 13), external forces and internal reactions are lumped at a finite number of points, *nodes*, along the line. By applying the equations of dynamic equilibrium and continuity to each mass, a set of discrete equations of motion is derived. Material damping, bending and torsional moments are normally neglected. Slack conditions were not investigated.

Finite Element Method

The FEM uses interpolation functions to describe the behaviour of a given variable internal to the element in terms of the displacements of the nodes defining the element. The equations of motion for a single element are obtained by applying the interpolation function to kinematic relations (strain/ displacement), constitution relations (stress/strain) and the equation of dynamic equilibrium.

It is demonstrated that computer codes based on FEM are slower compared with LMM.

Below we describe the **Numerical Model** at the basis of the application of the LMM.

Numerical Model

Line-end loads in the mooring line are: weight, buoyancy, sea floor reaction forces, line inertia, fluid loading. We assume that the motions of the structure, in the region of the surface wave frequency, are not affected by the mooring line tensions. The analysis of the wave frequency motions of the structure and the behaviour of the mooring line can be treated separately. The fluid load of the line is due to orbital velocities induced by waves, currents and line motions. This can be divided in components proportional to the relative fluid acceleration (*added inertia*) and proportional to the relative velocity square (*drag*). The "relative" adjective refers to the fact that the velocities are described along the mooring line and that the velocities and accelerations taken into account are the ones "seen" by the mooring line, so "relative" to the mooring line motion. The wave contribution to the relative velocity is normally small in comparison with the orbital velocity contribution and with the current and line motion contribution, therefore are neglected. It is preferable to describe the fluid loading in compo-

nents along the line (tangential) and in transverse (normal) direction, but bear in mind that the ultimate motions are required in earth-fixed "global" coordinates. In Fig. 14 we can see the nodal forces definition. The line to which the node belongs is the dashed-line, the normal (F_n) and tangential (F_t)component of the total force acting on the node, the buoyancy (B_j), the weight (G_j), the tension ($T_{(j-i)}$) transmitted from the previous node (therefore the index is j-1), the tension resulting from the calculation in the considered node (T_j), the directional matrix expressing the rotation with respect to the earth-fixed coordinate system ($\bar{\phi}_j$), the z and x axis are representing the earth-fixed coordinate system.

The mathematical model chosen is a modification of the LMM presented by Nakajima [18]. A computer program named DYNLINE, applies this method in two dimensions, assuming that the mooring line remains in the vertical plane through both line ends.
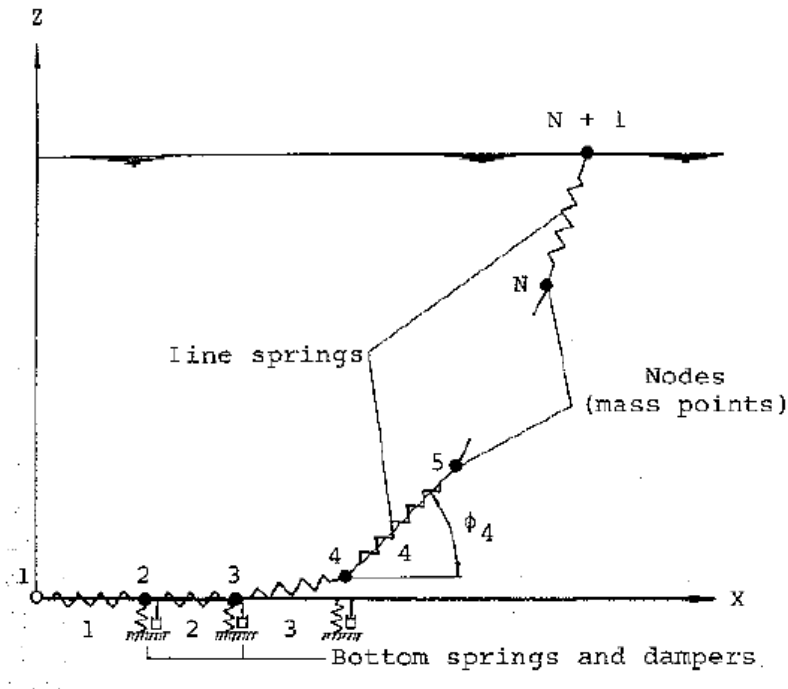

Figure 13: Discretization of mooring line by a LMM, the dots represent the lumped masses while the zigzag lines are the massless springs connecting the nodes. The co-ordinate system represented is earth−fixed. The bottom effect is simulated by spring-damped systems.

The space wise discretization of the mooring line is obtained by lumping all the forces to a finite number of nodes: *lumped masses*. The line is assumed to be fully flexible. The hydrodynamic forces are defined in the local system of coordinates (tangential and normal) to each mass. In order to derive the governing equations of motion fot the j-th lumped mass, Newton's law is written in earth−fixed coordinates:

$$[M_j + m_j(\tau)]\ddot{x}_j(\tau) = \underline{F}_j(\tau) \tag{1}$$

Where

j	indicates the lumped mass to which the equation refers
M_j	inertia matrix
m_j	added inertia
τ	time
$\underline{x}_j$	displacement vector
$\underline{F}_j$	external force vector

The *added inertia* matrix can be derived from normal and tangential fluid forces by directional transformations.

The nodal force vector $\underline{F}$ contains contributions from T (tension), F_D (drag force), F_W (weight and buoyancy), F_S (soil forces):

$$\underline{F}_j(\tau) = T_j(\tau)\underline{\Delta x}_j(\tau) - T_{j-1}(\tau)\underline{\Delta x}_{j-1}(\tau) + \underline{F_D}_j(\tau) + \underline{F_W}_j + \underline{F_S}_j(\tau) \tag{2}$$

Where

$\underline{\Delta x}_j$	segment basis vector $(\underline{x}_{j+1} - \underline{x}_j)/l_j$
l_j	original segment length

The *drag force* may be derived from the normal and tangential force components.

Sea floor contact may be simulated by spring-damped systems. Here are neglected tangential soil friction due to the big length of the line on the bottom and transverse soil reactive forces that are important in three dimensional problems.

The time domain relations between nodal displacements, velocities and accelerations may be approximated by the finite differential method such as the Houbolt scheme [19]. The segment *tension* $T_j(\tau + \Delta\tau)$ is derived from the node positions by a Newton-Raphson iteration.

In order to avoid instability and transient behaviour the simulation is started from an arbitrarily chosen state of equilibrium of the line. The simulation is started by applying starting functions to the upper-end boundary conditions. Knowing the inertia matrices and the right-hand side of Equation (1), the accelerations for the new time step are solved, consequently so are the displacements. A correction of tension is predicted. The whole procedure is repeated until an acceptable accuracy in tension is obtained. In that case the simulation is proceeded with the next time step by applying the next (in time) boundary condition.

Geometric discretization is an important aspect of the LMM method. The number of nodes should be sufficient to describe the line position. Moreover parasitical motions of lumped masses may occur. Neglecting the damping, the resonance frequencies of these parasitical motions may be approximated by:
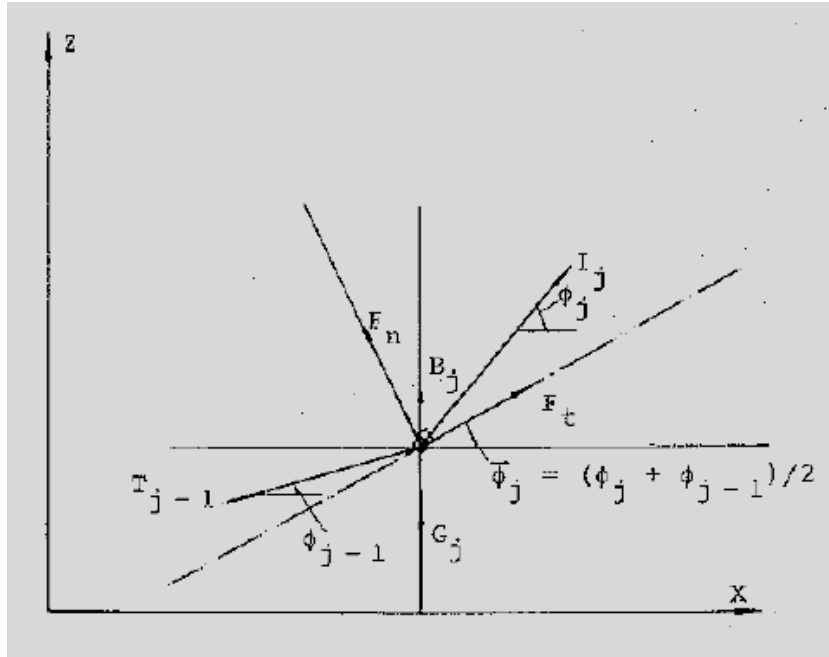
$$\omega_n = \sqrt{C(M+m)} \tag{3}$$

Where

Figure 14: Nodal Forces Definition in the system of coordinates along the mooring line (tangential and normal). The dashed-line is the line to which the node belongs. We can see the normal (F_n) and the tangential (F_t)component of the total force acting on the node, the buoyancy (B_j), the weight (G_j), the tension ($T_{(j-i)}$) transmitted from the previous node (therefore the index is j-1), the tension resulting from the calculation in the considered node (T_j), the directional matrix expressing the rotation with respect to the earth-fixed coordinate system ($\bar{\phi}_j$), the z and x axis are representing the earth-fixed coordinate system.

ω_n resonance frequency

C stiffness

M lumped mass

m added mass

For the usual types of moorings lines resonant response of separate masses in the lumped parameter model will not provide significant parasitical motions. The occurrence of such may be prevented by increasing the number of nodes, thus reducing the nodal mass and segment length.

Result of the present study show that in practical situations the dynamic behaviour of the mooring may contribute to the maximum tension significantly. Important parameters are the non-linear static load-excursion, the low frequency pre-tension and the amplitude and frequency of the exciting upper-end oscillation. At low frequencies the dynamic tension increases because of normal drag forces and gravity. Inertia becomes important at higher wave frequencies especially for steel wires and multi-component lines. For oscillations covering the taut situation of the line the dynamic amplification is small. Dynamic sea floor

reaction forces do not affect the behaviour of the line and can be modelled as critical damped springs to prevent numerical instabilities. It may be concluded that the use of the Lumped Mass Method does provide efficient and accurate predictions of dynamic motions and tension for offshore mooring analysis. The change of restoring force experienced by the floating structure is illustrated by an increase of amplitude of low frequency tension and phase shift. The dynamic behaviour of the mooring line may increase both the effective mooring stiffness and the low frequency damping.

The paper concluded with the following statements:

- The dynamic behaviour of mooring lines occurs in many practical offshore mooring situations and strongly increases the maximum line tension.

- The use of the Lumped Mass Method does provide efficient and accurate predictions of dynamic line motions and tensions certainly for engineering application.

- The dynamic components of mooring line tension may affect the low frequency motions of the moored structure by increase of the virtual stiffness and damping of the system.

3.3 Spectrum Analysis

This section describes the theoretical approach to model a surface mooring line used by Grosenbaugh [3]. In particular he proposes an analytical model for predicting the dynamics of instrumented oceanographic surface moorings made up of a combination of wire rope and compliant synthetic rope. In Fig. 15 we can see a taut and an inverse-catenary (for more details on these two types of design see Sec. 3.1) surface moorings that can be modelled with the Grosenbaugh method. The model simplifies the problem by treating only the vertical motion of the buoy and the longitudinal motion of the mooring line and attached instruments. The choice of treating only the vertical motion, maybe is owing to the fact that the heave motion is the only one that includes all the dynamic coefficients, such as added mass, damping, restoring (not only due to the restoring force induced to the line below the buoy -as it would be in case of horizontal motion-, but also the restoring force due to the changing in buoyancy during the motions of the buoy). Grosenbaugh demonstrates that the simplified model captures all of the important dynamic effects and gives accurate predictions of the dynamic tension at the top of the mooring line. The model shows that the *total mass* and *damping* of the instruments and wire rope of the mooring are the major sources of dynamic tension.

Below we briefly describe the Grosenbaugh analytical model and the solution.

Analytical Model

The difficult part of the analysis is to properly account for the effects of all the different components that make up the mooring. Dynamic tensions became a concern over the last few years because of the numerous failures due to fatigue of oceanographic moorings. The analytical model presented here simplifies the prediction of the dynamic response of oceanographic surface moorings and it is an excellent tool for the early stages of the design process. Different from previous studies, Grosenbaugh takes into consideration the effects of the wire rope, instruments and floating buoy apart from the nylon influence. It will be shown that the mass and the damping of the instruments controls the magnitude of the dynamic tension. Elastic strain of the wire and synthetic rope are important anyway. As already said, only heave motion of the buoy and the longitudinal motion of the instruments and mooring line will be taken into consideration to study the dynamic tensions. The longitudinal motions are maintained by the hydrodynamic damping all the way down the mooring line except for the inverse-catenary mooring in slack current conditions when the loop is present between the polypropylene and nylon ropes. The other major assumption of the model is that the dynamics of the instruments and their connecting hardware can be combined into a single point mass and damper that hangs just below the buoy, as illustrated in Fig. 16 (this reminds us of the approach used by Van den Boom [2]).

The instruments are typically located within the top few hundred meters of the mooring. The assumption is that the whole instrument string moves as a single unit with the same amplitude and phase of the surface buoy. Consequently, the dynamic tension at the buoy is effected only by the sum of the mass, added mass, and viscous damping of the instruments.
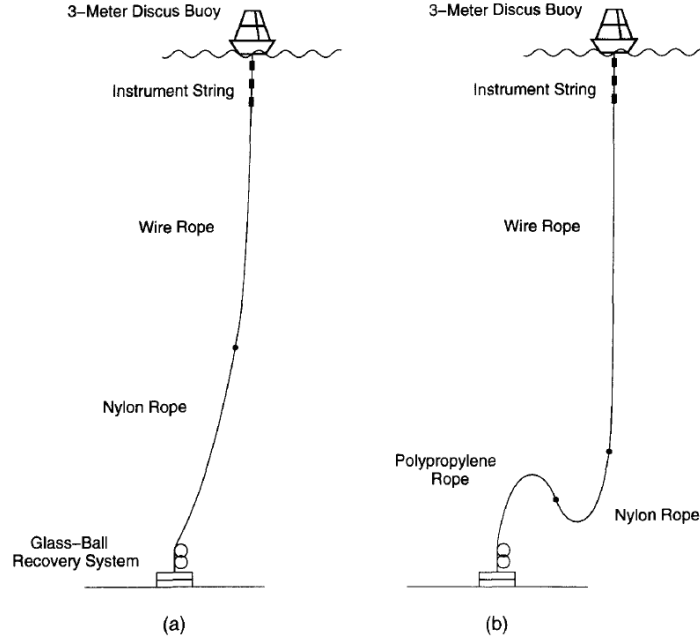
Figure 15: (a) Represents a taut oceanographic surface mooring, with attached instruments, wire rope in the top half of the mooring and a lower section of nylon rope. This is a Woods Hole Oceanographic Institution design of the 1960s; here wire rope is used in the upper 1500-2000 m to avoid instrument inclinations bigger than 15°and to prevent damages due to fish bites. The lower part of the mooring is made of nylon, so that the mooring can stretch without developing large tensions. (b) Represents an inverse-catenary mooring. This is a National Data Buoy Center design, developed in 1985 for offshore weather mooring.

The system is then represented with three coupled differential equations: one describing the heave motion of the buoy (equation (4)), one describing the vertical motion of the instruments (equation (5)) and one describing the longitudinal motion of the combination wire rope/synthetic rope mooring line (equation (9)and (10)).

The response of the buoy to a sinusoidal surface wave of the form $\tilde{\eta}e^{i\omega t}$ is governed by:

$$(M + M_{33})\frac{d^2U}{dt^2} + B_{33}\frac{dU}{dt} + C_{33}U = F_{33}(\tilde{\eta}e^{i\omega t}) - T \qquad (4)$$
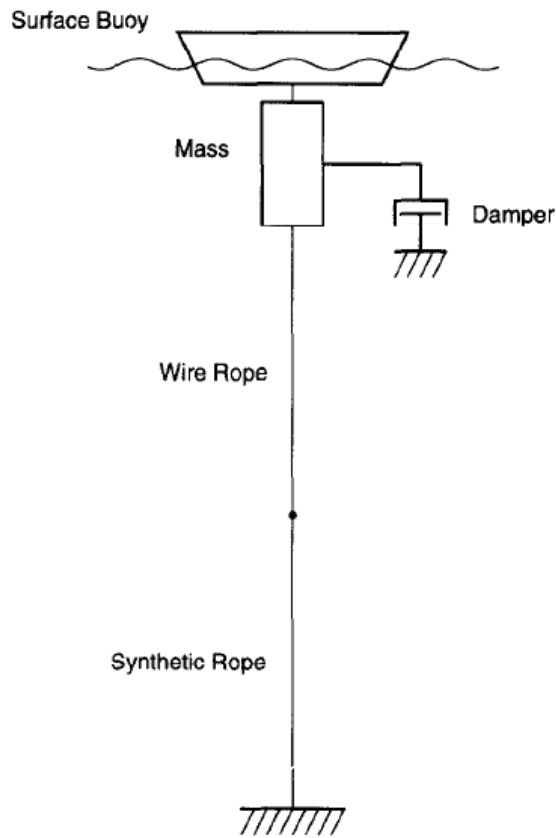
Where

Figure 16: This is the idealized model of an oceanographic surface mooring constituted of synthetic and wire rope and of in-line instruments. In the Fig. can be distinguished the concentrated mass and damper just below the buoy. The damper represent the sum effect of the attached instruments.

U	heave motion (displacement) of the buoy
M	mass of the buoy
M_{33}	added mass in heave
B_{33}	heave damping coefficient
C_{33}	heave restoring force of the buoy
F_{33}	vertical wave exciting force per unit of wave amplitude
$\tilde{\eta}$	wave amplitude
ω	wave frequency
T	dynamic tension at the top of the mooring line
i	$\sqrt{-1}$
t	time

The added mass, wave damping coefficients and wave force, that are all frequency dependent are calculated using the potential theory ([20]).

Vertical motion of the instrument string:

$$(\tilde{M} + \tilde{M}_a)\frac{d^2\tilde{U}}{dt^2} + \tilde{B}\frac{d\tilde{U}}{dt} = (T - T_0) \tag{5}$$

Where

$\tilde{M}$ sum of the mass of the instruments plus any wire rope, chain and steel mooring hardware that are used to connect the instruments together

$\tilde{M}_a$ sum of the added mass of the instruments and connecting hardware

$\tilde{U}$ vertical motion of the instrument string.

$\tilde{B}$ equivalent linearised drag coefficient that represents the sum of the viscous drag forces of the instruments and connecting hardware

T_0 dynamic tension just beneath the point mass

The damping term $\tilde{B}$ is found by a linearisation process for irregular seas.

$$\tilde{B} = \sum (\frac{2}{\pi})^{\frac{1}{2}} \rho \tilde{C}_j \tilde{A}_j \sigma_{\dot{U}} \tag{6}$$

Where

$\tilde{C}_j$ quadratic drag coefficient of the jth mooring component

$\tilde{A}_j$ characteristic area

$\sigma_{\dot{U}}$ standard deviation of the velocity of the vertical motion of the instrument string

Assuming zero strain in the instrument string, the vertical motion of the instruments and the heave motion of the buoy have the same amplitude and phase:

$$\tilde{U} = U \tag{7}$$

$$\sigma_{\dot{\tilde{U}}} = \sigma_{\dot{U}} \tag{8}$$

Longitudinal motion of the wire/synthetic rope line:

Wire rope: $L_s \leq z \leq L_s + L_w$

$$m_w \frac{\partial^2 u}{\partial t^2} + b_w \frac{\partial u}{\partial t} = E_w A_w \frac{\partial^2 u}{\partial z^2} \tag{9}$$

Synthetic rope: $0 \leq z \leq L_s$

$$m_s \frac{\partial^2 u}{\partial t^2} + b_s \frac{\partial u}{\partial t} = E_s A_s \frac{\partial^2 u}{\partial z^2} \tag{10}$$

Where

u(z)	longitudinal motion (displacement) of a mooring line
m	mass per unit of length
b	equivalent linearised damping coefficient per unit length
E	Young's modulus
A	cross-sectional area of the respective material
z	distance along the mooring line
L_w	overall length of the wire rope
L_s	overall length of the synthetic rope

The boundary conditions at the top and bottom of the mooring line are:

$$u(0) = 0 \tag{11}$$

$$u(L_s + L_w) = \tilde{U} \tag{12}$$

At the junction between wire rope and synthetic rope the displacements and the tensions are required to be continuous:

$$u(L_s^-) = u(L_s^+) \tag{13}$$

$$E_s A_s \frac{\partial u}{\partial z}\big|_{z=L_s^-} = E_w A_w \frac{\partial u}{\partial z}\big|_{z=L_s^+} \tag{14}$$

So the tension at the top of the wire just below the point mass is given by:

$$T_0 = E_w A_w \frac{\partial u}{\partial z}\big|_{z=L_s+L_w} \tag{15}$$

The Solution

The solution is presented in terms of transfer functions which give the response per unit wave amplitude for a wave of frequency ω. These are obtained by assuming that the dependent variables are sinusoidal. After solving the differential equations for the wire and synthetic rope mooring line and applying the boundary conditions, it is possible to find the transfer function $H_u(\omega)$ for the heave motion of the buoy, that is:

$$H_u(\omega) = \frac{F_{33}}{C_{33} - M_{\sum}\omega^2 + iB_{\sum}\omega + \alpha(E_s A_s k_s \cot k_s L_s - E_w A_w k_w \tan k_w L_w)} \tag{16}$$

Where

$$M_{\sum} = M + M_{33} + \tilde{M} + \tilde{M}_a$$

sum of the mass and added mass of the buoy and of the instrument string

$$B_{\sum} = M_{33} + \tilde{M}$$

sum of the damping of the buoy and of the instrument string

More over:

$$\alpha = (1 + \frac{E_s A_s k_s}{E_w A_w k_w} \cot k_s L_s \tan k_w L_w)^{-1} \qquad (17)$$

The elastic wave number of the wire (k_s) and of synthetic ropes (k_w) is:

$$k_w = (\frac{m_w \omega^2 - i b_w \omega}{E_w A_w})^{\frac{1}{2}} \qquad (18)$$

$$k_s = (\frac{m_s \omega^2 - i b_s \omega}{E_s A_s})^{\frac{1}{2}} \qquad (19)$$

Given the transfer function of the buoy motion, we can calculate the frequency domain response corresponding to a given sea state from:

$$S_U(\omega) = |H_U(\omega)|^2 S_\eta(\omega) \qquad (20)$$

$S_U(\omega)$ power spectrum of the buoy motion
$S_\eta(\omega)$ is the wave amplitude power spectrum of a particular sea state.

$S_\eta(\omega)$ can be calculated for example with a Bretschneider wave spectrum [4]. To do this we need to know the significant height of the waves and the period of zero crossing of the part of the ocean we are interested in. We can find this data for example in a wave atlas such as the Global Wave Statistics [22]. Grosenbaugh uses a Pierson-Moskowitz wave spectrum [5], for which we only need to know the wind velocity.

Because the damping of the instrument string and the mooring line depend on their longitudinal motion (initially unknown), the solution has to be calculated by iteration. At the beginning of the process, the amplitude of the heave motion at every point on the mooring is set equal to the wave amplitude $\tilde{\eta}$, so that the standard deviation of the velocity of the motion is equal to the standard deviation of the velocity of the wave surface $\sigma_{\dot{\eta}}$. Substituting this value for $\sigma_{\dot{U}}$ in equation (6) and for $\sigma_{\dot{U}}(z)$ in the analogous equations for the linearised damping coefficients per unit of length of the wire and synthetic rope (not reported here) it is possible to obtain new values of $\sigma_{\dot{U}}$ and $\sigma_{\dot{u}}(z)$ from:

$$\sigma_{\dot{U}} = (\int_0^\infty \omega^2 S_U(\omega) d\omega)^{\frac{1}{2}} \qquad (21)$$

$$\sigma_{\dot{u}}(z) = (\int_0^\infty \omega^2 S_u(\omega, z) d\omega)^{\frac{1}{2}} \qquad (22)$$

Here $S_u(z, \omega)$ is the power spectrum of the longitudinal motion at a given point on the mooring line. The new values of $\sigma_{\dot{U}}$ and $\sigma_{\dot{u}}(z)$ are substituted back

---

[4]The **Bretschneider wave spectrum** is a two parameter spectrum. It is used to define, in case of open sea, both the spectrum of a fully developed sea and of a developing/extinguishing sea [21]. It can be expressed by the relation: $S_\eta^B(\omega) = \frac{A}{\omega^5} e^{-\frac{B}{\omega^4}}$.

[5]The **Pierson-Moskowitz wave spectrum** is a one parameter spectrum, aimed at representing a fully developed sea, resulting from a prolonged wind without swell wave influence. The model is based on North Atlantic wave records. [21]. This spectrum is defined by $S_\eta(\omega) = \frac{\alpha g^2}{\omega^5} e^{(-\beta(g/V_w \omega))}$.

into equation (6) and in the analogous equations for the linearised damping coefficients per unit of length of the wire and synthetic rope and a new solution is found, until convergence is achieved.

To validate this study, Grosenbaugh reports comparisons with full-scale measurements numerical simulation (see in Fig. (18)) [3]. In Fig. (17) we can see the hydrodynamic coefficient used by Grosenbaugh for a 3 m of diameter discus buoy.
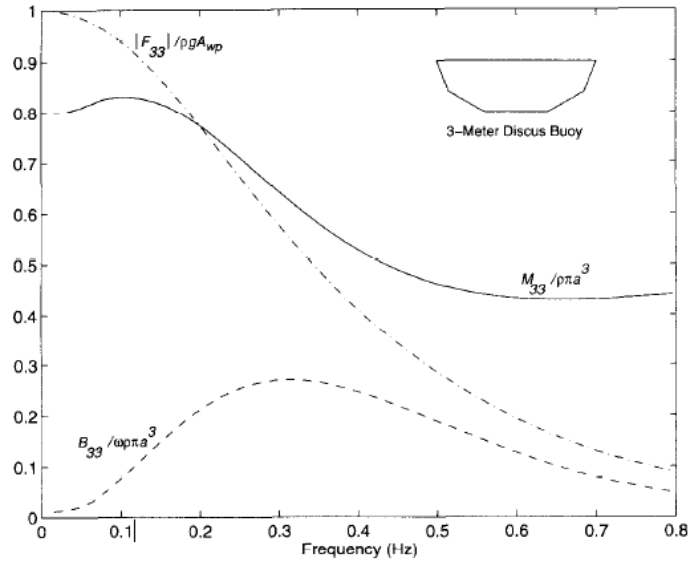

Figure 17: Hydrodynamic heave coefficients and wave exciting force of the 3-m discus buoy. The added mass (M_{33}) and wave damping (B_{33})curves are normalized by $\rho\pi a^3$ where ρ is the water density and a is the radius of the water plane. The water plane is meant as the horizontal plane defined from the wet perimeter of the floating buoy. The wave exciting force curve (F_{33}) is non-dimensionalized by the heave restoring force $\rho g \pi a^2$. On the x-axis there is the frequency [Hz]. [3]

The analytical model shows explicitly the individual effects of the instruments, mooring hardware, wire rope and synthetic rope that go into the overall dynamic response. This is important to engineers in the early phases of the design process when it is being decided how many instruments and how much wire and synthetic rope will be used in the mooring.

Measurements showed that the total mass and damping of the instruments, hardware, chain, and wire rope that made up the stiff upper half of the mooring were the major sources of the dynamic tension. Damping of the instruments becomes a significant factor in larger sea states, especially near the peak frequency of the wave spectrum. In large sea states, the damping forces can be twice as large as the inertial forces near the peak frequency. In the smaller sea states, this relationship is reversed.
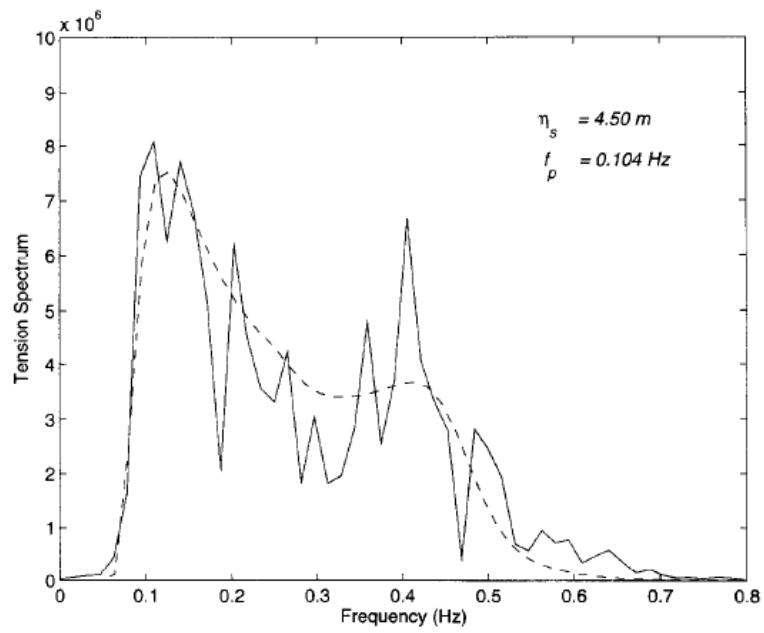
Figure 18: Comparison between measured tension power spectra (solid line) for a taut mooring and predictions based on the analytical model (dashed line) for the given fully-developed sea state. On the y-axes there is the tension spectrum. On the x-axis there is the frequency [Hz]. η_s is the significant height of the wave and f_p is the frequency of the peak of the wave [3].

3.4 The Boundary Value Problem Method

This is one of the theoretical approaches to the dynamical problem regarding a floating object [4]. The first step in setting the BVP is to divide the boundary of a certain volume of fluid (including the free surface) in a finite number of segments. Through this method it is possible to write a set of equations to calculate the velocity potential, in such a way that the partial derivatives for each direction gives the velocity in that direction. Some of these equations describe the potential calculated on every segment of the space others are the description of the boundary conditions that we have set (e.g the radiation condition at the vertical wall of the material region). Solving the written set of equations allows us to find the velocity potential, therefore the velocity field, the pressures and the forces.

In case of a perfect, incompressible, irrotational fluid, the continuity equation can be written like:

$$\nabla^2 \phi = 0 \tag{23}$$

This is known as the Laplace Equation, where ϕ is the velocity potential. This relation is valid on all of the considered volume of fluid (V). The flow of the vectorial quantity $[\phi \nabla \varphi - \varphi \nabla \phi]$ through the surface of a box of volume of fluid can be written, using Green's Theorem, as the integral over the volume of the divergence of the same vectorial quantity:

$$\int_{S_V} [\phi \nabla \varphi - \varphi \nabla \phi] \cdot \vec{n} dS = \int_V \nabla \cdot [\phi \nabla \varphi - \varphi \nabla \phi] dV \tag{24}$$

The integral over the volume is zero, since both ϕ and φ satisfy Laplace's equation, so:

$$\int_{S_V} [\phi \nabla \varphi - \varphi \nabla \phi] \cdot \vec{n} dS = 0 \tag{25}$$

$$\int_{S_V} [\phi \frac{\partial \varphi}{\partial n} - \varphi \frac{\partial \phi}{\partial n}] dS = 0 \tag{26}$$

Using this property it is possible to solve this integro-differential equation on the surface of V, extracting ϕ and using a source/sink for φ, called Green's function. In this way the number of unknowns will be reduced from N^3 (obtained from the discretization of volume) to $6 \times N^2$.

It can be demonstrated that the integro-differential equation, with a Green's function φ for 3D cases $\varphi = \frac{1}{r}$ becomes:

$$\int_{S_V} [\phi \frac{\partial}{\partial n} (\frac{1}{r}) - (\frac{1}{r}) \frac{\partial \phi}{\partial n}] dS = -2\pi \phi \tag{27}$$

Where r is the distance between the point in which the potential ϕ needs to be calculated and the generic integration point.

In the 2D case, as Green function can be used $\Phi = \log(r)$ and

$$\int_{S_V} [\phi \frac{\partial}{\partial n} (\log(r)) - (\log(r)) \frac{\partial \phi}{\partial n}] dS = -\pi \phi \tag{28}$$

In the 2D case, the integration surface is a closed line. To compute the integral, the line is divided in N segments and on each segment the integral is evaluated. The second Green Identity becomes:

$$\sum_{j=1}^{N} \int_{S_V} [\phi_j \frac{\partial}{\partial n}(\log(r_{ij})) - (\log(r_{ij}))\frac{\partial \phi}{\partial n}]dS_j = -\pi\phi_i \tag{29}$$

Where subscript i indicates the segment on which point P lays (generally at the centre of the segment), where the potential ϕ_i is calculated. Subscript j indicates the generic segment in which the integral is calculated. S_j represents the surface of the generic j segment and r_{ij} represents the distance between the point P and the generic point of integration, as we can see in Fig. 19.
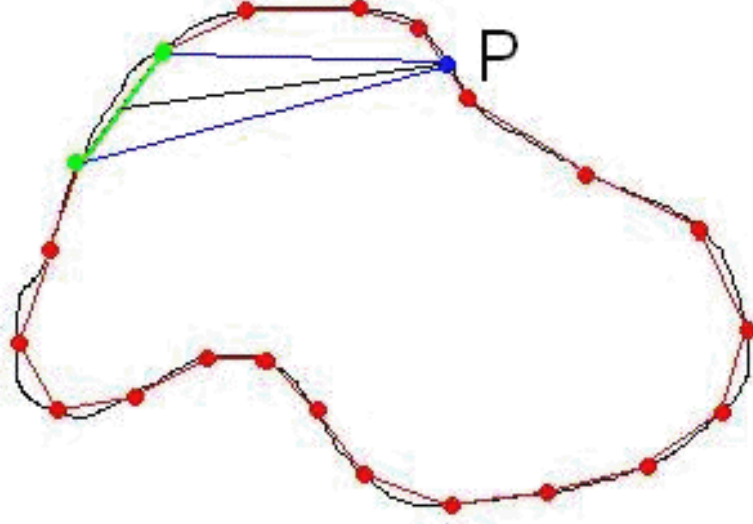
Figure 19: The surface of integration for the 2D case of the Boundary Value Problem is a closed line. A method of integration consists in dividing the line in several segments, in order to calculate on each of these the integral and then use the additive property of the integral. P represent the point in which the potential ϕ_i is going to be calculated. Source [4].

If ϕ_j and $\frac{\partial \phi}{\partial n}|_j$ are considered constant they can be removed from the integral:

$$\sum_{j=1}^{N} \phi_j \int_{s_j} [\frac{\partial}{\partial n}(\log(r_{ij}))_i]dS - \sum_{j=1}^{N} \frac{\partial \phi}{\partial n}|_j \int_{S_j} \log(r_{ij})dS_j = -\pi\phi_i \tag{30}$$

Now the terms within the integral [kernels] depend just on geometrical quantities and can be calculated analytically. Writing N equations, one for every point P (each containing 2 integrals) at the end there are N equations and 2N unknowns (ϕ_i and $\frac{\partial \phi}{\partial n}|_j$). Setting N boundary conditions prescribing ϕ_i or $\frac{\partial \phi}{\partial n}|_j$

there will be 2N equations and 2N unknowns and the system can be solved. Typically the boundary conditions are [23]:

- Kinematic boundary condition on the Surface

- Dynamic boundary condition on the Surface

- Sea Bed boundary condition

- Continuity condition

- Radiation condition

Kinematic boundary condition on the Surface
The velocity of a water particle at a point at the surface of the body is equal to the velocity of this body point itself
Dynamic boundary condition on the Surface
The pressure at the free surface of the fluid is equal to the atmospheric pressure.
Sea Bed boundary condition
The vertical velocity of water particles at the sea bed is zero
Continuity condition
Irrotationality implies that the water particles in the three translational directions, follow from the gradient of the velocity potential Φ (Laplace condition):

$$u = \frac{\partial \Phi}{\partial x}$$

$$v = \frac{\partial \Phi}{\partial y}$$

$$w = \frac{\partial \Phi}{\partial z}$$

Radiation condition
The radiation condition states that as the distance from the oscillating body becomes large, the potential value tends to zero. In Fig. 20 we can see the boundary conditions described above.
On the sea bottom an upward arrow indicates the normal direction ($\vec{n}$) and the formula: $\vec{V} \cdot \vec{n} = \nabla \phi \cdot \vec{n} = \frac{\partial \phi}{\partial n} = 0$ indicates the sea bed impermeability boundary condition (where $\vec{V}$ is the velocity vector, ϕ the velocity potential, $\vec{n}$ the normal velocity vector).
The walls of the pool are periodic: $\phi(X, t) = \phi(X + \lambda, t)$ or $\phi(X, t) = \phi(X, t + T)$ where T is the period and X is the distance covered by the considered regular wave).
The free surface shows the dynamic ($\eta = -\frac{1}{g} \cdot \frac{\partial \phi}{\partial t}|_{Y=0}$) and kinematic ($\frac{\partial \eta}{\partial t} = \frac{\partial \phi}{\partial Z}|_{Y=0}$) conditions, where η is the wave elevation.
In this figure the radiation condition doesn't show up because in this case the frame work is a pool and we are interested in avoiding wave reflection effects in the mathematical model, therefore the condition imposes the wave to behave as if the wall wasn't there.
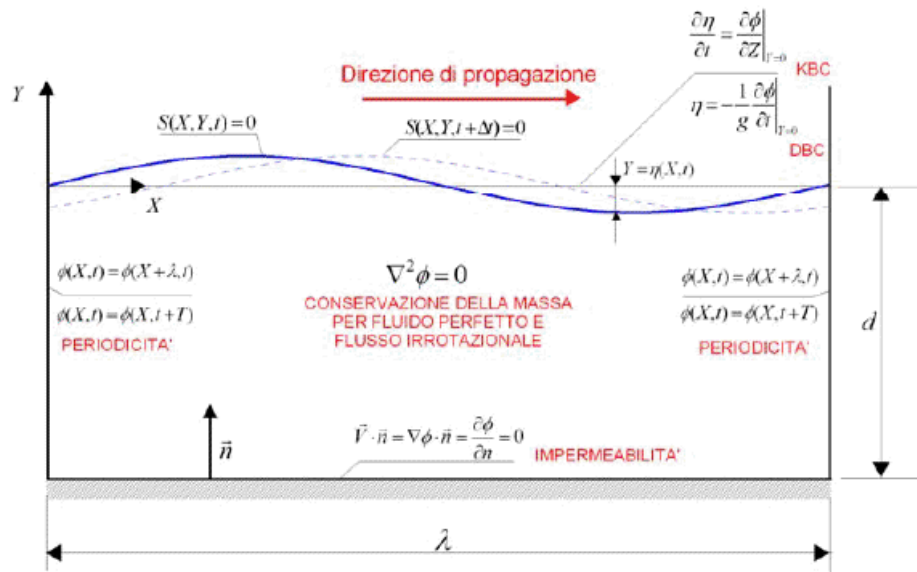
Figure 20: The figure shows the boundary conditions described in the text. The vertical axes represents Y. The blue line indicates the shape of the free surface, that in this case indicates one wave length (λ).

On the sea bottom: ($\vec{n}$) indicates the normal direction and $\vec{V}\vec{n} = \nabla\phi \cdot \vec{n} = \frac{\partial\phi}{\partial n} = 0$ indicates the sea bed impermeability boundary condition.

The walls of the pool are periodic: $\phi(X,t) = \phi(X + \lambda, t)$ or $\phi(X,t) = \phi(X, t + T)$.

The free surface shows the dynamic ($\eta = -\frac{1}{g} \cdot \frac{\partial\phi}{\partial t}|_{Y=0}$) and kinematic ($\frac{\partial\eta}{\partial t} = \frac{\partial\phi}{\partial Z}|_{Y=0}$) conditions.

See the text for equations explanations. Source [4].

4 Mooring & Design Dynamics

Mooring Design and Dynamics is a set of Matlab routines that can be used to assist in the design and configuration of single point oceanographic moorings, the evaluation of mooring tension and shape under the influence of wind and currents, and the simulation of mooring component positions when forced by time dependent currents. The static model will predict the tension and tilt at each mooring component, including the anchor, for which the safe mass will be evaluated in terms of the vertical and horizontal tensions. Predictions can be saved to facilitate mooring motion correction.

Mathematical features

The "model" part of MD&D (moordyn.m) solves the positions of each mooring element using an iterative process. The first iteration (solution) starts with the mooring standing vertically in the water column. Once the first estimation of the tilted mooring has been made, new solutions are sought with the updated positions of each element in the sheared current used to re-calculate the local drag, considering tilted elements and appropriate exposed surface area. It considers also a certain stretching of the rope/wire. If the position of the top element (usually a float, or at least a positively buoyant instrument) moves less than 1 cm between successive iterations, then it is assumed the solution has converged and the position of the mooring has been found. Inertia is not considered, nor is vibration or snap loading. The solutions, even for time dependent simulations, are all assumed to be (locally) "static". To set the environmental conditions The program asks a small depth array made up at least of three elements representing the depth at which the currents have been measured. MDD also assumes that the first given value is the depth of the water in which the mooring will work. Therefore for surface moorings, the top (highest) velocity value defines the water depth. A density profile, and even a time dependent density profile may be entered, as the drag depends on the water density. A constant wind can be set that produces an additional 2 % surface current in the direction of the wind. Modify the wind direction if you want to simulate Ekman veering [24][6] which decreases linearly to a depth that increases with wind speed. The model will predict if the surface float gets "dragged" under the surface by the currents [1].

NON-Dynamic Movie

The MDD offers the possibility to build a "movie" showing the positions of the mooring line through time. To do this time dependent current data are necessary. More in detail the arrays to insert in the program are: t (time), w (time dependent current component upwards), v (time dependent current component northwards), u (time dependent current component eastwards), z (considered depths). Once time dependent currents have been entered a sequence of static positions, depending from the current associated at each time step, can be displayed in a movie. It has to be noticed that even if the input data are time-

---

[6]

Ekman spiral effect(see Fig. 21)
Ekman observed that the direction of the current over the depth of the Ekman layer, differs by a clockwise turning of $\sim 40°$ (in the Northern Hemisphere). If we want to simulate this effect we have to set the direction of the wind changed from reality of $\sim 40°$ to the right since we are in the north hemisphere. The depth (D) of the Ekman layer is given by:
$D = \sqrt{(\frac{k}{f})}$, where k is a term depending from viscosity and f is the Coriolis parameter.
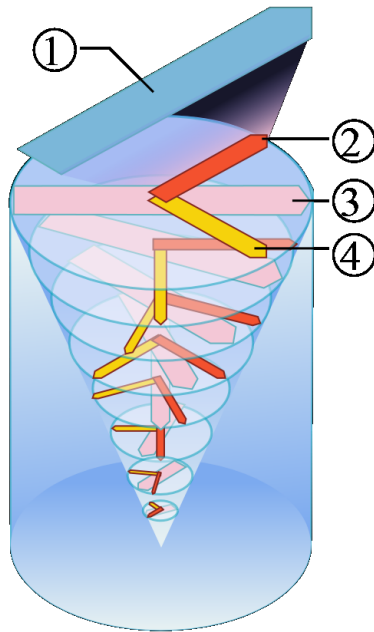
Figure 21: Ekman spiral effect. In the figure: 1. wind, 2. force from above, 3. effective direction of the current, 4. Coriolis effect.[24]

dependent the program doesn't take into consideration the dynamic loads as added mass and damping, hence the name "non-dynamic". The movie is actually built through a series of photos, each representing the position of the line end of the buoy due to static loads, which, however, are changing at every time step.

5 WHOI Cable

Implementation features WHOI Cable is a suite of applications, all of which are centred around the primary solver program, *cable*.
The used version is the **2.0**.
The modelled system can consist of any combination of different cable, chain, and rope segments, with instruments, floats, and connectors between segments. For a given model system, a single input file is used to define numerical settings, environmental parameters, system components, and system geometry. The main post-processing program is *animate*. Solutions for three-dimensional problems can be drawn and animated. WHOI Cable includes post-processors to convert results to binary Matlab format or to ASCII text files (*res2mat* or *res2asc*).
animate reads cable results files directly and can produce animations showing system spatial configuration in conjunction with the spatial distribution of force, moment and velocity quantities along the cable and/or the temporal distribution of these quantities.
res2mat reads the available results information in the cable output file and writes a Matlab (.mat) file containing symbolically named variables for all of the results.
The post-processing application *res2asc* can be used to convert binary cable results to tabular ASCII data. Each of the result matrices are saved to separate files. The primary interface under Windows is an encapsulator that provides a graphical interface to all of the component programs. The animation post-processor is written for the X Window environment.

Mathematical features

For all problem types the governing differential equations for WHOI Cable include bending stiffness, material non-linearities, coordinate transformation based on Euler parameters, and a model for cable-bottom interaction. These features provide important new capabilities compared to previous software programs used for modelling oceanographic cable structures.

Numerical features

For both static and dynamic problems, the mathematical problem is posed as a system of coupled, non-linear partial differential equations. At each step of the problem the discretized system of non-linear equations is solved by an iterative, implicit, adaptive relaxation technique [7] The initial guess for the solution in static problems is calculated using a shooting method. For the dynamic solution, the initial guess at each time step is the solution from the previous time step.

Notation and coordinate system

The origin of the basic coordinate system (see Fig. 22) is always located at the anchor and the global z direction is positive upwards, global x is positive to the right, and global y is positive into the page. Current can be defined as a function of depth and can flow in both the x and y directions. Currents with vertical components (along the z axis) are not allowed. All of the component

---

[7]In mathematical optimization, relaxation is a modelling strategy. A relaxation is an approximation of a difficult problem by a nearby problem that is easier to solve. A solution of the relaxed problem provides information about the original problem. The primary non-linear solution technique within *cable* is known as relaxation. Using an initial guess as a solution vector, the algorithm calculates an update to the solution that will bring the system closer to equilibrium. The updated solution is then fed back into the algorithm and the process repeats until some suitably close approximation of equilibrium is achieved [25].

programs are written in the C programming language. The input language for cable is meant to be flexible and immediate.

Concerning the relationship between the various *cable* components under Windows see Fig. 23.
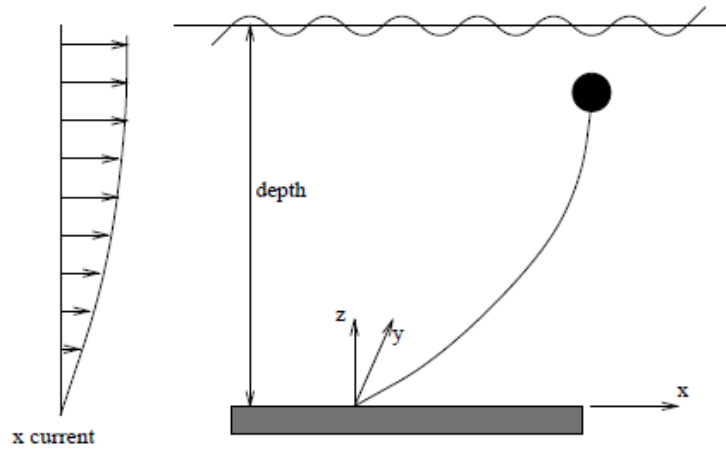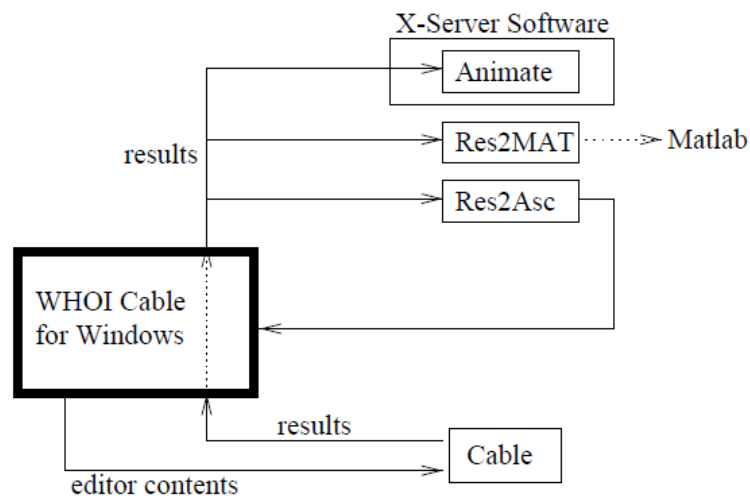

Figure 22: Cable Coordinate system [25]

Figure 23: *Cable*'s Window interface, i.e. the relationship between the various *cable* component programs under Windows [25]. The user communicates with the program through a single interface which communicates with the heart program (*cable*). The results can be converted, depending on the needs of the user, to a Matlab file (through the *Res2MAT*) containing symbolically named variables for all of the results, or to tabular ASCII data (through the *Res2Asc*). Each of the result matrices are saved to separate files. As can be seen in the figure, post-processing options exist in the form of the animate application. *animate* reads cable results files directly and can produce animations showing system spatial configuration in conjunction with the spatial distribution of force, moment and velocity quantities along the cable and/or the temporal distribution of these quantities.

6 Data

The two main sources of data that we have been using in the design are Sea-DataNet web page [5] and The Scatter diagram kindly provided by Henk van den Boom (Head of Department, Trials & Monitoring, Marin).

SeaDataNet

Before starting looking for data we have to bear in mind that the spot of the ocean we are interested in is 40 West and 14 North and that the data that we need to define a current profile in this zone are ADCP (Acoustic Doppler Current Profiler) or current meter data. The main difference between the two is that the former gives us the measurement of the velocities along the water column, while the latter is giving us the measurement of velocity in a single point. Looking in the web page SeaDataNet we found some **current meter** measurements at the position (Fig. 24):

Longitude $[east] - 040.81$ (the minus indicates that the position is at west of Greenwich, that is in the Atlantic Ocean)
Latitude $[north] + 10.78$
Time of the measurements:
Start date: 20th October 1977
Start time: 1:50:00 (UT)
End date: 21st October 1977
End time: 00:00:00 (UT)
Water depth: 4990 (Close to our 5000 m)
Platform type: subsurface mooring
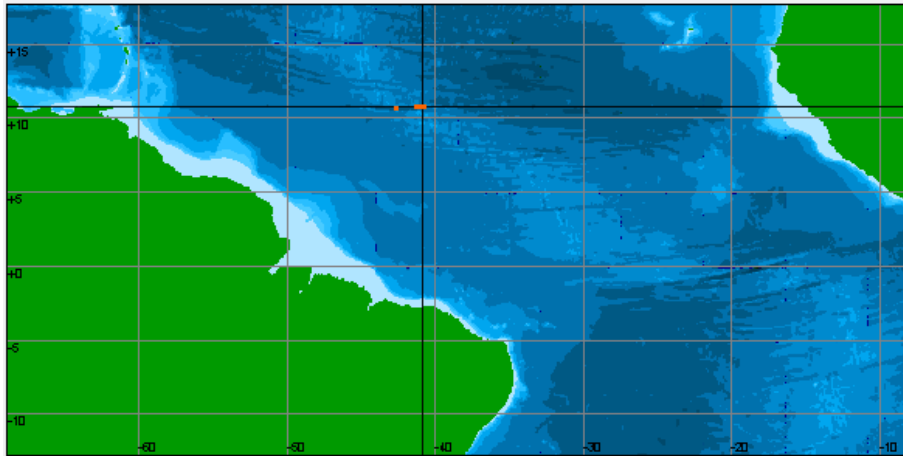Data Holding centre: IFREMER / IDM/SISMER

Figure 24: The position of the Ifremer (Institut français de recherche pour l'exploitation de la mer) subsurface mooring. [5]

Scatter Diagram

Here below in Fig. (25) we can find the scatter diagram of the location of the
sea we are interested in: 40 West 14 North. Based on 5 year data collection,
from ECMWF (European Centre for Medium-Range Weather Forecasts). The
graph above is a time series of wave height, below on the left there is the scatter
diagram of mean wave period and wave height and on the left the histogram of
the mean wave direction.

Looking at this data set we choose as design condition, to be used in the ENVI-
RONMENT section of *cable* input file (see Sec. 7.2), $H_s = 4m$ and $T_1 = 10s$, this
seems a good bases for this analysis, covering the most of the observations.
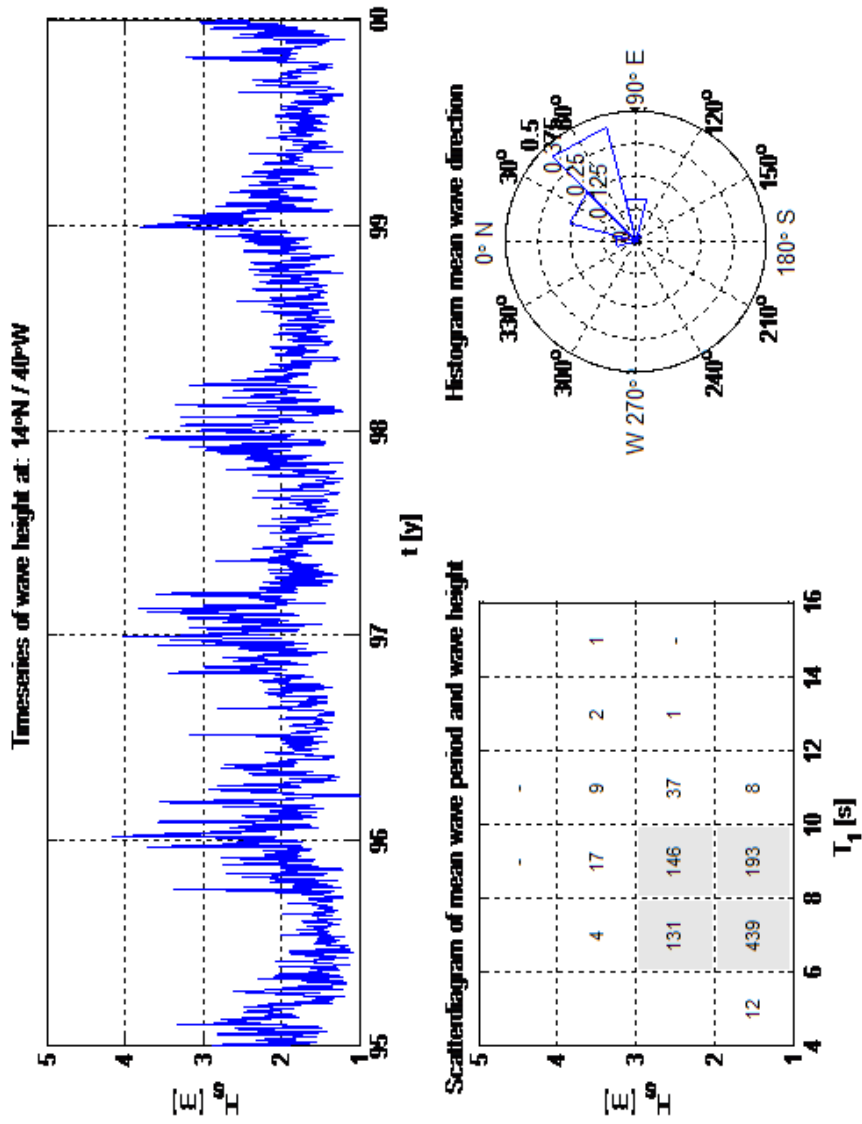
Figure 25: The scatter diagram of the location: 40 West 14 North. Based on 5 year data collection, from ECMWF. From the top we can see: time series of wave height (H_s); on the left: scatter digram of mean wave period (T_1) and wave height (H_s); right: histogram mean wave direction.

7 Methodology

According with what so far explained and after collecting all the necessary data, we can make the point of the situation before starting to compute a solution. Therefore here below we describe our choices as far as the **design option**, the **in-line instruments**, the **theoretic approach** and the **programs** are concerned.

Design option

A wire unstretchable part is necessary for the 3500 m sediment trap, this pinpoints the **hybrid solution**, that is the solution chosen for this design, even if the inverse catenary option seems to be the trend according to the contacted companies.

In-line instruments

Following the suggestions of the GEO department in collaboration with Marum we are going to use the **Dolan** buoy and the **Technicap** sediment traps (see Sec. 2.1 and 2.2). Near each sediment trap, following the GEO request we have to attach a current meter.

Theoretic approach

The **BVP** seems to be a coherent choice considering my study path and can be helpful in the understanding of the problem.

Programs

First we will face the design from a statical point of view with **MDD** and then from a dynamical point of view with **Cable**.

7.1 MDD Procedure

Facing the design through MDD we have to take in account some parameters as:

- How to get the S shape

- The worst case scenario in which the mooring will work

- The maximum breaking tension of the wire

- How to maintain the position of the instruments

- How to avoid inclinations bigger than 15 deg.

For the single passages within Matlab we cross reference to the MDD user Guide [1]. After some attempts we found the right combination of buoyancy, wire and synthetic rope to obtain in slack current conditions (see Fig. 28) the S shape and to maintain the desired position for the instruments. As we add new in-line elements the program displays in the Matlab command window the list of the chosen instruments, their length, buoyancy and position along the line (see Fig. 26). After evaluating the built mooring is possible to display its shape, Fig. 27 is reliable only as far as the shape of the line is concerned but doesn't tell us anything about the position of the instruments in line after the evaluation, this information is displayed in the Matlab command window, as we see Fig. 29, here this time we can read also the height of the middle point of the instrument, its coordinate in the hearth fixed system of reference, having the origin at the bottom of the anchor, the tensions at the top and at the bottom of each element and their inclination.

Its also possible to obtain a plot of the main in line instruments as in Fig. 30 but the drown mooring is not scale drawing .

After setting the lay out of the mooring we can compare the in-line tensions with the breaking tension of the wire. As we can see Fig. 31, as far as the tensions are concerned the mooring is not failing in slack current. so we can test it in the worst case scenario, choosing the higher values of currents among the data available for our region.

```
   In-Line
 # Mooring Element    Length[m] Buoy[kg] Height[m]
                                          (top)
 1 DOLAN                  0.04  2009.50   6334.41
 2 1/2" buoy chain        5.00    -3.07   6334.37
 3 3T SeineSwivel         0.11    -0.65   6329.37
 4 3/8 wire rope        800.00    -0.33   6329.26
 5 3T SeineSwivel         0.11    -0.65   5529.26
 6 3/8 wire rope        400.00    -0.33   5529.16
 7 5/16 Crosby           0.05    -0.34   5129.16
 8 Instr. Top            0.55    -2.30   5129.11
 9 Aanderaa RCM-11       0.60   -18.00   5128.56
10 Instr. bottom         0.32    -1.06   5127.96
11 Instr. Top            0.55    -2.30   5127.64
12 Techn.pps52           2.30   -32.00   5127.09
13 Instr. bottom         0.32    -1.06   5124.79
14 5/16 Crosby           0.05    -0.34   5124.47
15 3T SeineSwivel        0.11    -0.65   5124.42
16 1 Nylon            1500.00    -0.00   5124.31
17 3T SeineSwivel        0.11    -0.65   3624.31
18 3/4 Polyprop       1610.00     0.02   3624.21
19 3T SeineSwivel        0.11    -0.65   2014.20
20 3/4 Polyprop        500.00     0.02   2014.10
21 5/16 Crosby           0.05    -0.34   1514.10
22 CRP1500/250           1.00   250.00   1514.05
23 5/16 Crosby           0.05    -0.34   1513.05
24 Instr. Top            0.55    -2.30   1513.00
25 Aanderaa RCM-11       0.60   -18.00   1512.45
26 Instr. bottom         0.32    -1.06   1511.85
27 Instr. Top            0.55    -2.30   1511.53
28 Techn.pps52           2.30   -32.00   1510.98
29 Instr. bottom         0.32    -1.06   1508.68
30 5/16 Crosby           0.05    -0.34   1508.36
31 CRP1500/250           1.00   250.00   1508.31
32 5/16 Crosby           0.05    -0.34   1507.31
33 3/8 wire rope      1500.00    -0.33   1507.26
34 5/16 Crosby           0.05    -0.34      7.26
35 CRP1500/100           0.80    97.00      7.21
36 5/16 Crosby           0.05    -0.34      6.41
37 double AR-191         0.85   -60.00      6.36
38 Thiele 2              0.21    -0.74      5.51
39 1/2 chain SL          5.00    -4.12      5.30
40 KM3 3000 kg           0.30 -3000.00      0.30
```

Figure 26: In line instruments displayed by MDD. The first column represent the name that the program gives to every component, the second column shows the length of each instrument, the third indicates the buoyancy (negative is toward the bottom), the last column tells us which is the position along the line of the top point of every instrument.
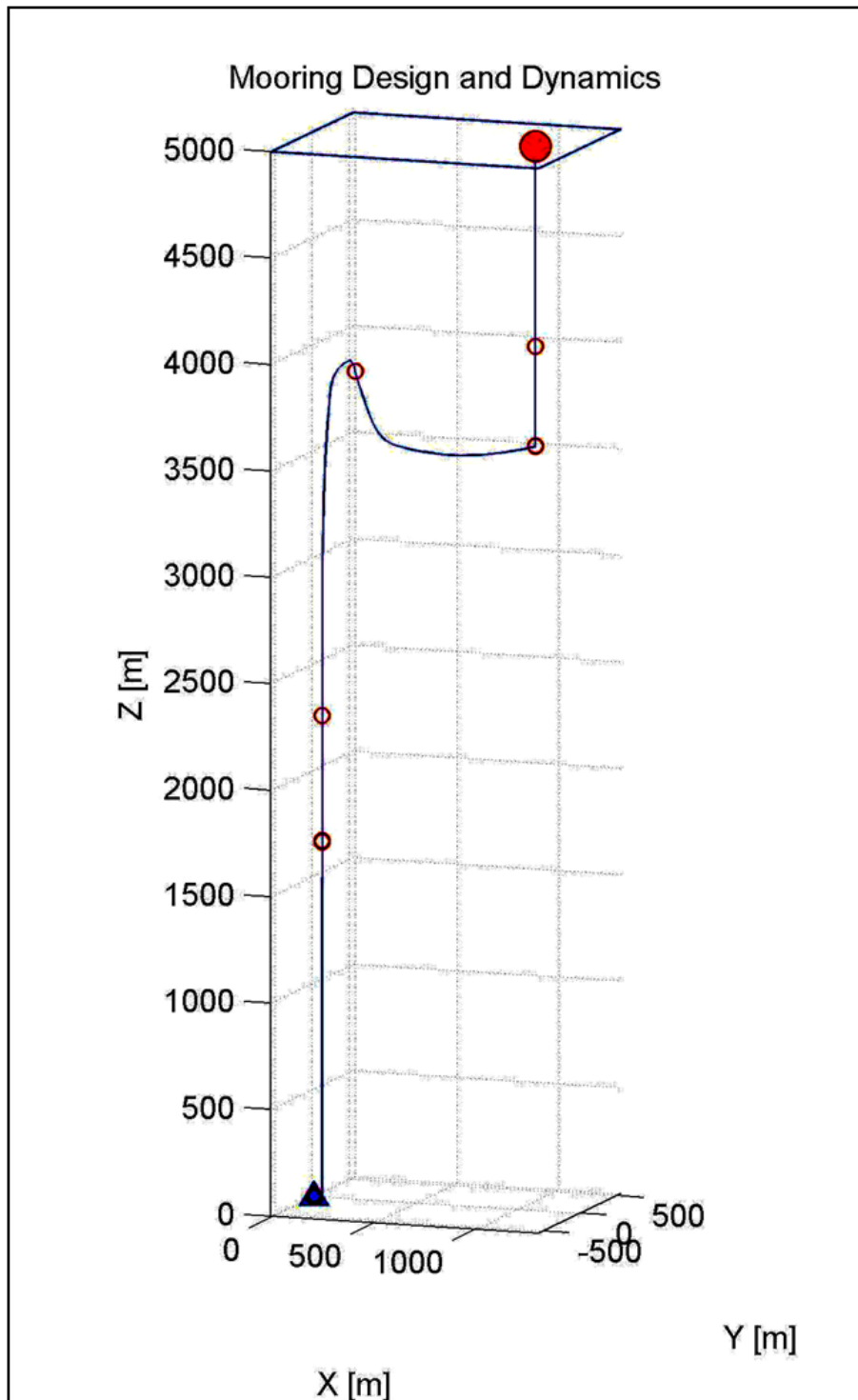
Figure 27: S shape obtained according with MDD, the figure is reliable only as far as the shape of the line is concerned but doesn't tell us anything about the instruments in line.

Height[m]	U [m/s]	V [m/s]	W [m/s]	Density [kg/m^3]
5000.00	0.00	0.00	0.00	1024.00
2000.00	0.00	0.00	0.00	1025.00
0.00	0.00	0.00	0.00	1026.00

Figure 28: The three component of velocities u (eastwards), v(northwards) and w (upwards) are set to zero for three chosen depth (5000 ,2000, 0 m) for the first evaluation.

	In-Line							Tension[kg]		Angle[deg]	
#	Mooring Element	Length[m]	Buoy[kg]	Height[m] (middle)	dZ[m]	dX[m]	dY[m]	Top	Bottom	Top	Bottom
1	DOLAN	0.04	2009.50	5000.01	-651.0	916.4	0.0	0.0	470.7	0.0	0.0
2	1/2" buoy chain	5.00	-3.07					470.7	455.3	0.0	0.0
3	3T SeineSwivel	0.11	-0.65	4994.07	-650.2	916.4	0.0	455.3	454.7	0.0	0.0
4	3/8 wire rope	800.29	-0.33					454.7	190.7	0.0	0.0
5	3T SeineSwivel	0.11	-0.65	4056.80	-513.3	916.4	0.0	190.7	190.0	0.0	0.0
6	3/8 wire rope	400.06	-0.33					190.0	58.0	0.0	0.0
7	5/16 Crosby	0.05	-0.34	3588.24	-444.9	916.4	0.0	58.0	57.7	0.0	0.0
8	Instr. Top	0.55	-2.30	3587.89	-444.8	916.4	0.0	57.7	55.4	0.0	0.0
9	Aanderaa RCM-11	0.60	-18.00	3587.22	-444.7	916.4	0.0	55.4	37.4	0.0	0.0
10	Instr. bottom	0.32	-1.06	3586.68	-444.6	916.4	0.0	37.4	36.3	0.0	0.0
11	Instr. Top	0.55	-2.30	3586.17	-444.6	916.4	0.0	36.3	34.0	0.0	0.0
12	Techn.pps52	2.30	-32.00	3584.50	-444.3	916.4	0.0	34.0	2.0	0.0	0.0
13	Instr. bottom	0.32	-1.06	3582.97	-444.1	916.4	0.0	2.0	1.0	0.0	3.9
14	5/16 Crosby	0.05	-0.34	3582.75	-444.0	916.4	0.0	1.0	0.7	3.9	6.2
15	3T SeineSwivel	0.11	-0.65	3582.67	-444.0	916.4	0.0	0.7	0.2	6.2	82.4
16	1 Nylon	1500.02	-0.00					0.2	0.2	82.4	157.2
17	3T SeineSwivel	0.11	-0.65	3987.48	-596.3	72.2	0.0	0.2	0.8	157.2	180.0
18	3/4 Polyprop	1612.08	0.02					0.8	24.9	180.0	0.0
19	3T SeineSwivel	0.11	-0.65	2272.94	-331.9	36.2	0.0	24.9	24.3	0.0	0.0
20	3/4 Polyprop	501.42	0.02					24.3	32.3	0.0	0.0
21	5/16 Crosby	0.05	-0.34	1685.69	-246.2	36.2	0.0	32.3	31.9	0.0	0.0
22	CRP1500/250	1.00	250.00	1685.08	-246.1	36.2	0.0	31.9	281.9	0.0	0.0
23	5/16 Crosby	0.05	-0.34	1684.46	-246.0	36.2	0.0	281.9	281.6	0.0	0.0
24	Instr. Top	0.55	-2.30	1684.11	-245.9	36.2	0.0	281.6	279.3	0.0	0.0
25	Aanderaa RCM-11	0.60	-18.00	1683.44	-245.8	36.2	0.0	279.3	261.3	0.0	0.0
26	Instr. bottom	0.32	-1.06	1682.90	-245.8	36.2	0.0	261.3	260.2	0.0	0.0
27	Instr. Top	0.55	-2.30	1682.39	-245.7	36.2	0.0	260.2	257.9	0.0	0.0
28	Techn.pps52	2.30	-32.00	1680.72	-245.4	36.2	0.0	257.9	225.9	0.0	0.0
29	Instr. bottom	0.32	-1.06	1679.19	-245.2	36.2	0.0	225.9	224.9	0.0	0.0
30	5/16 Crosby	0.05	-0.34	1678.97	-245.2	36.2	0.0	224.9	224.5	0.0	0.0
31	CRP1500/250	1.00	250.00	1678.36	-245.1	36.2	0.0	224.5	474.5	0.0	0.0
32	5/16 Crosby	0.05	-0.34	1677.74	-245.0	36.2	0.0	474.5	474.2	0.0	0.0
33	3/8 wire rope	1500.41	-0.33					474.2	20.8	0.0	180.0
34	5/16 Crosby	0.05	-0.34	4.54	-0.8	0.9	0.0	20.8	21.2	180.0	180.0
35	CRP1500/100	0.80	97.00	5.04	-0.9	0.9	0.0	21.2	75.8	180.0	0.0
36	5/16 Crosby	0.05	-0.34	5.48	-0.9	0.9	0.0	75.8	75.5	0.0	0.0
37	double AR-191	0.85	-60.00	4.95	-0.8	0.9	0.0	75.5	15.5	0.0	0.0
38	Thiele 2	0.21	-0.74	4.33	-0.7	0.9	0.0	15.5	14.8	0.0	0.0
39	1/2 chain SL	5.00	-4.12					14.8	5.8	0.0	180.0
40	KM3 3000 kg	0.30	-3000.00	0.18	-0.1	0.0	0.0	5.8	180.0		

Figure 29: The first three columns are the same as in Fig. 26, the fourth represents the height of the middle point of each instrument, the fifth its coordinate in the hearth fixed system of reference, having the origin at the bottom of the anchor, and then the last two show the tensions at the top and at the bottom of each element and their inclination.
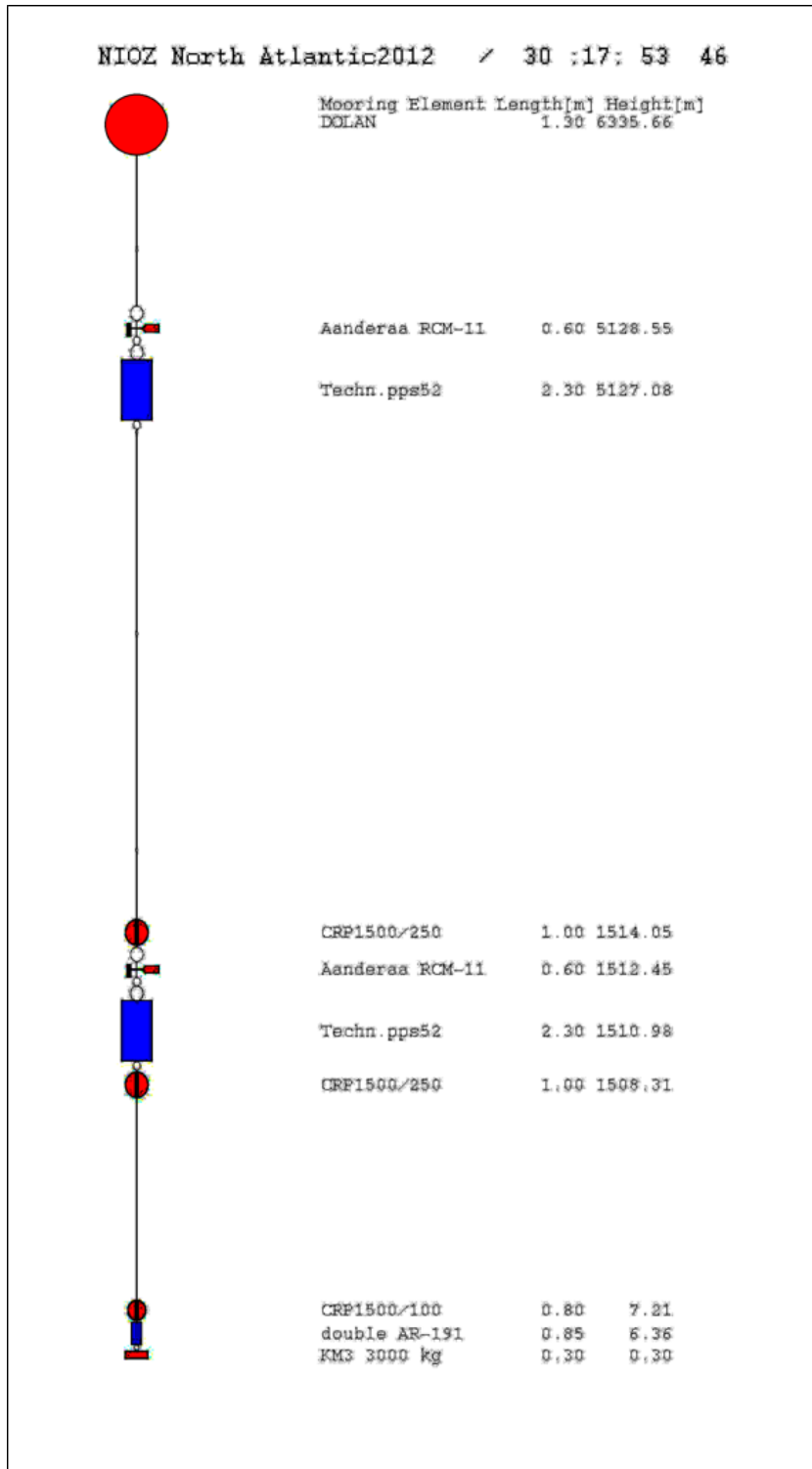
Mooring Element	Length[m]	Height[m]
DOLAN	1.30	6335.66
Aanderaa RCM-11	0.60	5128.55
Techn.pps52	2.30	5127.08
CRP1500/250	1.00	1514.05
Aanderaa RCM-11	0.60	1512.45
Techn.pps52	2.30	1510.98
CRP1500/250	1.00	1508.31
CRP1500/100	0.80	7.21
double AR-191	0.85	6.36
KM3 3000 kg	0.30	0.30

NIOZ North Atlantic2012 / 30 ;17: 53 46

Figure 30: The aim of this plot is to show the main in line instruments. It is not scale drawing.
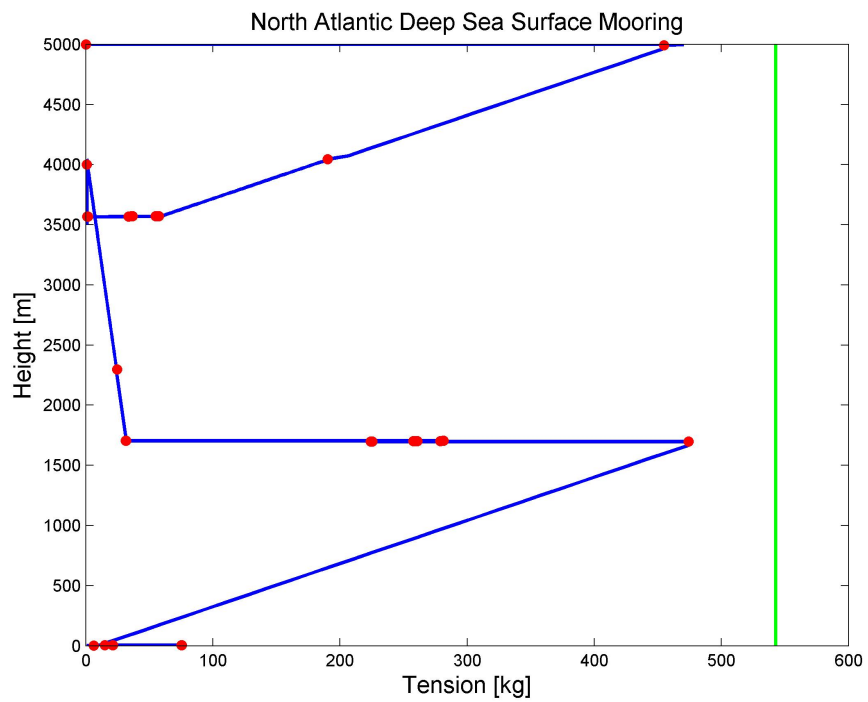
Figure 31: Comparison between in-line tensions in slack conditions and breaking tension. On the x-axis we can see the tension in Kg. On the y-axis we can see height of the mooring in the water. The green line represents the break tension of the wire. The blue the tensions along the line. The red spots are the positions of the dust collectors, the anchor and of the buoys.

So we can test it in the worst case scenario, choosing the higher values of currents among the data available for our region (see Fig. 32) is important to notice that the w value is non realistic for the bottom and the middle depth, there is no flow across the bottom and the vertical velocity value can be close to the horizontal velocity value only near the surface in deep waters. As easily foreseeable the S shape is now gone and the tensions changed (see Fig. 33 and 34).

U [m/s]	V [m/s]	W [m/s]	Density [kg/m^3]
0.16	0.03	0.17	1024.00

Figure 32: These are the three higher components of current velocity. Here the depth is not displayed because the current is considered that strong along all the water column. Here is important to notice that the w value is non realistic for the bottom and the middle depth.

Is then possible to compare the tensions in this case with the breaking tension of the wire, we can see in Fig. 35 that the mooring is still working as the blue line (tensions along the mooring) doesn't cross the green one (breaking tension).
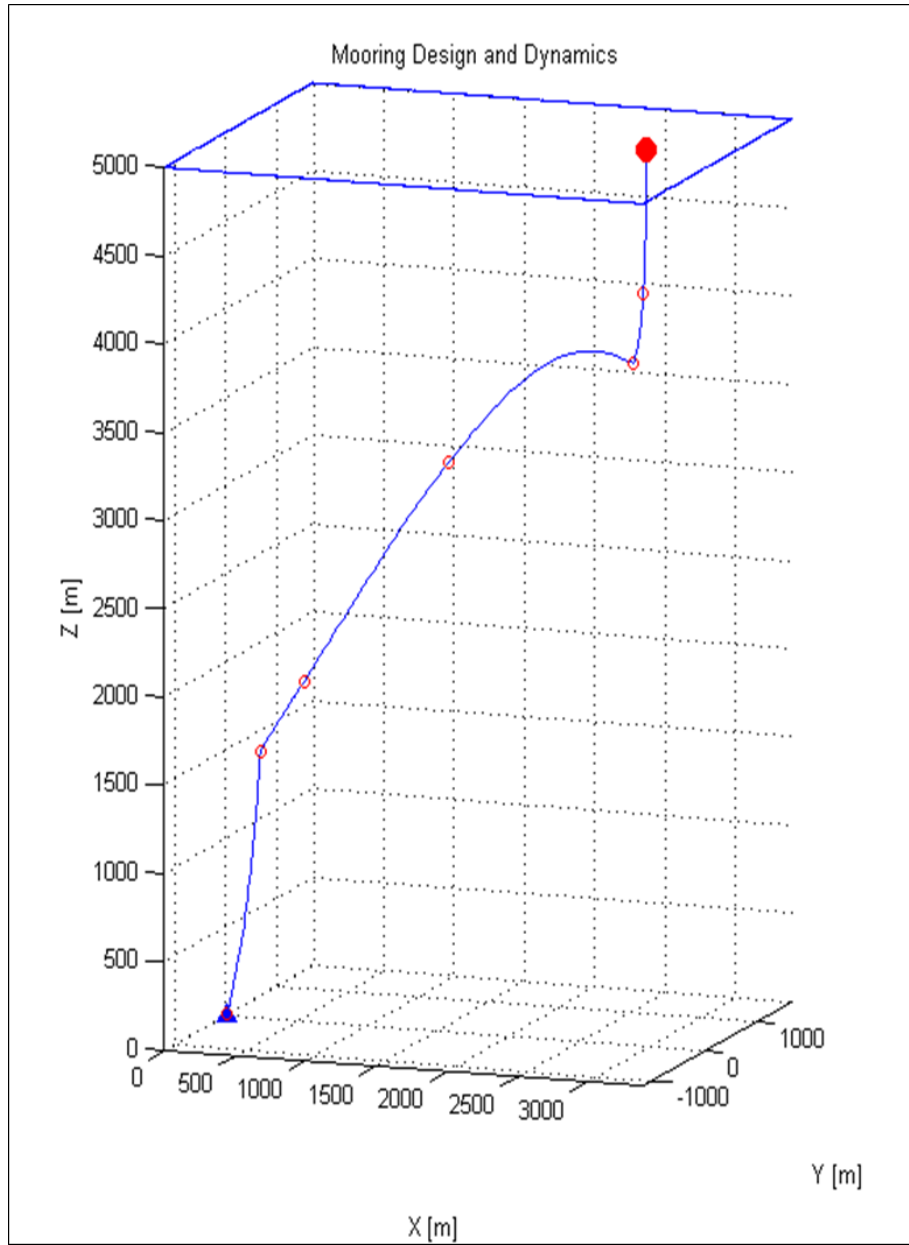
Figure 33: With strong currents the S shape is not visible any more.

# Mooring Element	Length[m]	Buoy[kg]	Height[m] (middle)	dZ[m]	dX[m]	dY[m]	Tension[kg] Top	Bottom	Angle[deg] Top	Bottom
1 DOLAN	0.04	2009.50	5000.01	-494.6	2952.0	433.8	0.0	458.6	0.0	0.0
2 1/2" buoy chain	5.00	-3.07					458.6	443.3	0.0	0.0
3 3T SeineSwivel	0.11	-0.65	4994.59	-494.2	2952.0	433.8	443.3	442.6	0.0	0.0
4 3/8 wire rope	800.28	-0.33					442.6	178.8	0.0	4.7
5 3T SeineSwivel	0.11	-0.65	4140.03	-440.1	2931.6	430.9	178.8	178.1	4.7	4.7
6 3/8 wire rope	400.05	-0.33					178.1	49.3	4.7	28.8
7 5/16 Crosby	0.05	-0.34	3725.21	-425.4	2852.6	419.5	49.3	49.0	28.8	29.0
8 Instr. Top	0.55	-2.30	3724.93	-425.4	2852.5	419.5	49.0	47.1	29.0	30.3
9 Aanderaa RCM-11	0.60	-18.00	3724.41	-425.5	2852.2	419.5	47.1	33.1	30.3	46.1
10 Instr. bottom	0.32	-1.06	3724.02	-425.5	2851.9	419.4	33.1	32.4	46.1	47.4
11 Instr. Top	0.55	-2.30	3723.71	-425.7	2851.6	419.4	32.4	30.9	47.4	50.4
12 Techn.pps52	2.30	-32.00	3722.75	-426.1	2850.6	419.3	30.9	24.4	50.4	109.3
13 Instr. bottom	0.32	-1.06	3722.04	-426.7	2849.6	419.1	24.4	24.8	109.3	111.4
14 5/16 Crosby	0.05	-0.34	3722.10	-426.9	2849.4	419.1	24.8	24.9	111.4	112.1
15 3T SeineSwivel	0.11	-0.65	3722.13	-427.0	2849.4	419.1	24.9	25.1	112.1	113.3
16 1 Nylon	1503.19	-0.00					25.1	31.8	113.3	43.7
17 3T SeineSwivel	0.11	-0.65	3282.26	132.0	1590.4	235.3	31.8	31.3	43.7	44.9
18 3/4 Polyprop	1616.83	0.02					31.3	53.3	44.9	32.0
19 3T SeineSwivel	0.11	-0.65	1905.03	36.0	705.7	105.2	53.3	52.8	32.0	32.5
20 3/4 Polyprop	502.82	0.02					52.8	59.6	32.5	32.5
21 5/16 Crosby	0.05	-0.34	1453.48	-14.0	442.6	66.3	59.6	59.3	32.5	32.7
22 CRP1500/250	1.00	250.00	1453.01	-14.0	442.4	66.2	59.3	301.7	32.7	5.6
23 5/16 Crosby	0.05	-0.34	1452.54	-14.1	442.1	66.2	301.7	301.4	5.6	5.6
24 Instr. Top	0.55	-2.30	1452.22	-14.0	442.1	66.2	301.4	299.1	5.6	5.6
25 Aanderaa RCM-11	0.60	-18.00	1451.61	-14.0	442.0	66.2	299.1	281.2	5.6	6.0
26 Instr. bottom	0.32	-1.06	1451.12	-14.0	442.0	66.2	281.2	280.1	6.0	6.0
27 Instr. Top	0.55	-2.30	1450.66	-13.9	441.9	66.2	280.1	277.8	6.0	6.1
28 Techn.pps52	2.30	-32.00	1449.14	-13.9	441.8	66.1	277.8	246.1	6.1	8.2
29 Instr. bottom	0.32	-1.06	1447.75	-13.8	441.6	66.1	246.1	245.0	8.2	8.3
30 5/16 Crosby	0.05	-0.34	1447.56	-13.8	441.6	66.1	245.0	244.7	8.3	8.3
31 CRP1500/250	1.00	250.00	1447.00	-13.7	441.5	66.1	244.7	493.4	8.3	4.1
32 5/16 Crosby	0.05	-0.34	1446.45	-13.7	441.5	66.1	493.4	493.1	4.1	4.1
33 3/8 wire rope	1500.46	-0.33					493.1	56.5	4.1	94.5
34 5/16 Crosby	0.05	-0.34	2.94	0.9	6.0	0.9	56.5	56.5	94.5	94.6
35 CRP1500/100	0.80	97.00	2.98	1.3	5.6	0.8	56.5	106.8	94.6	30.9
36 5/16 Crosby	0.05	-0.34	2.99	1.7	5.2	0.8	106.8	106.5	30.9	31.0
37 double AR-191	0.85	-60.00	2.58	1.6	5.0	0.7	106.5	64.1	31.0	61.4
38 Thiele 2	0.21	-0.74	2.14	1.6	4.7	0.7	64.1	63.8	61.4	62.0
39 1/2 chain SL	5.00	-4.12					63.8	57.2	62.0	79.5
40 KM3 3000 kg	0.30	-3000.00	0.16	-0.0	0.0	0.0	57.2		79.5	

Figure 34: The first three columns are the same as in Fig. 26, the fourth represents the height of the middle point of each instrument, the fifth its coordinate in the hearth fixed system of reference, having the origin at the bottom of the anchor, and then the last two show the tensions at the top and at the bottom of each element and their inclination.
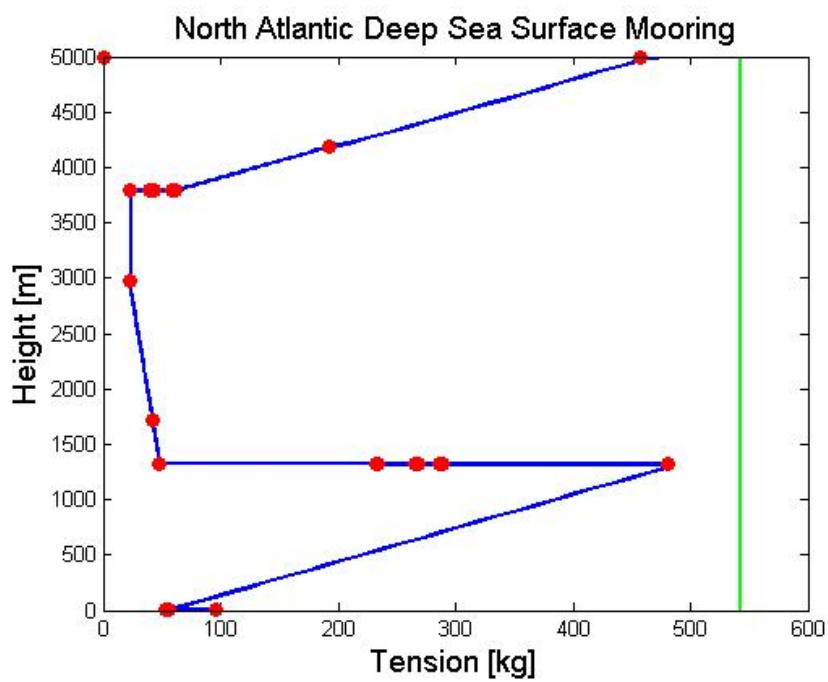
Figure 35: Comparison between in-line tensions in worst case scenario and breaking tension. On the x-axis we can see the tension in Kg. On the y-axis we can see height of the mooring in the water. The green line represents the break tension of the wire. The blue the tensions along the line. The red spots are the positions of the dust collectors, the anchor and of the buoys.

7.2 Cable procedure

Input file

Since the data base of *cable* is not wide as the one of MDD and adding new elements require a deep knowledge of the technical specification of every instrument, for the moment we focus on the ropes segments.

Before starting to build our mooring with Cable through the Windows interface we need to know that an input file is constituted by eight main sections. (The TYPEWRITER font is used to indicate key words that belong in input files):

- PROBLEM DESCRIPTION: contains the most basic description of the system.

- ANALYSIS PARAMETER: contains definitions that control the numerical algorithms which are used in the solution of *cable* problems. The solution can be split in two main phases: dynamic and static.

- ENVIRONMENT: this section is used to define the external conditions under which the simulation is run.

- BUOYS: this section defines the buoy that is used at the top of the mooring. In our this case remind that we will use the Dolan buoy (see Sec. (2.1))

- ANCHORS: defines the anchors that are used at one or both ends of the system. We only create a valid anchor name to be used in the terminal definitions of the layout section.

- CONNECTORS: used to define the shackles, floats, and instruments that are placed between cable segments. A connector is defined by a unique name followed by a series of property definitions.

- MATERIALS: defines the cable materials that make-up the system. Each material definition consists of a unique name followed by a series of material property definitions.

- LAYOUT: here the geometry of the most model systems is built from the bottom up as a series of segments with optional connectors between segments and terminal points at the ends. Terminal points can consist either of buoys or anchors. Note that in Dewey Matlab application Mooring Design & Dynamic is the opposite, i.e. the first element is always the buoy in case of moorings.

We refer only to our mooring without listing all the options allowed by the program, for which we cross-refer to the Cable Guide [25]. Here below we report the input file in Window with the relative comment:

PROBLEM DESCRIPTION

TITLE = "NIOZ NORTH ATLANTIC" is a character string containing the problem title to be used in the display of results.

TYPE = SURFACE is the problem type.

ANALYSIS PARAMETERS

STATIC-OUTER-ITERATIONS = 1000 is the maximum permitted number of iterations to take in resolving the anchor or buoy position in the static solution.

STATIC-ITERATIONS = 5000 is the maximum permitted number of relaxation iterations in the static solution.

STATIC-RELAXATION = 0.1 is the relaxation factor to be used in the static solution. Many static problems are only stable with a relaxation factor of 0.1 or smaller.

STATIC-TOLERANCE = 0.001 is the convergence tolerance for static iterations.

STATIC-OUTER-TOLERANCE = 0.01 is the convergence tolerance for the outer loop of static iterations.

DURATION = 400.0 is the total length of the dynamic simulation.

TIME-STEP = 0.1 is the time step of the dynamic simulation.

DYNAMIC-TOLERANCE = 1e-6 is the convergence tolerance for dynamic iterations. The best choice for this parameter is almost always 1.0.

DYNAMIC-RELAXATION = 1.0 is the relaxation factor to be used in the dynamic solution.

DYNAMIC-ITERATIONS = 20 is the maximum permitted number of relaxation iterations at each time step. A value of 20 is appropriate for most problems.

RAMP-TIME = 50.0 is the time period over which the excitation amplitudes will be linearly ramped up to their full values. It is generally advisable to ramp the excitation over one or two excitation or wave periods.

ENVIRONMENT

RHO = 1025 is the density of the fluid medium. Must always be specified.

GRAVITY = 9.81 is the acceleration of gravity expressed in appropriate units. Must always be specified.

X-CURRENT = (0.0, 0.1640) (100, 0.1640) (1000, 0.1640) (5000, 0.1640) is the current in the global x-direction, possibly as a function of depth. Since we used current meter measurements (Fig. 36), the x-current that we know is not a function of depth, but only of time so we choose the strongest current. (see Sec. 6)

DEPTH = 5000 is the depth of the water.

INPUT-TYPE = RANDOM it specifies the nature of the dynamic inputs. RANDOM inputs build a random profile using the given amplitude as the significant amplitude and the given period as the peak period.

FORCING-METHOD = WAVE-FOLLOWER this must be specified for dynamic problems. WAVE-FOLLOWER means that with wave following surface buoys the heave motion of the buoy is governed by the instantaneous vertical displacement of the wave field defined by X-WAVE= and Y-WAVE= or WAVE-FILE=. The buoy is free to respond to time-varying forcing by current.

X-WAVE = (2.0, 10.0, 0.0) is the amplitude, period, and relative phase of the surface wave travelling in the global X direction. We choose these values taking into account the scatter diagram reported in Fig. 25 and discussed in Sec. 6

BOTTOM-STIFFNESS = 0.0 is the spring stiffness of the bottom per unit length.

BOTTOM-DAMPING = 0.0 is the damping ratio of the bottom.

BUOYS

FLOAT is the name that we are going to use in the LAYOUT section.

TYPE = CYLINDER is the basic buoy type.

M = 1500 is the mass of the buoy.

D = 2.4 is the diameter of the buoy for buoy shapes with pre-defined geometry (this is our case).

$C_{dn} = 1.0$ is the normal drag coefficient of the buoy.

ANCHORS

CLUMP is the name that we are going to use in the LAYOUT section.

CONNECTORS

SHACKLE is the name that we are going to use in the LAYOUT section.

D = 0.375 * 0.0254 is the characteristic diameter used to calculate a drag area.

WET = 8.0 is the wet weight of the connector.

$C_{dn} = 0.1$ is the normal drag coefficient of the connector.

M = 1.0 is the mass of the connector .

SSF is the name that we are going to use in the LAYOUT section.
D = 1.628
M = 931.3
WET = −13350
$C_{dn} = 2.068$

MATERIALS

WIRE

EA $= 4.4e6$ is the axial stiffness of the material. Must be non-zero. For ropes and cables this value should typically be less than the straight product of E (elastic modulus) times A (cross-sectional area).

EI $= 500$ is the bending stiffness of the material. Must be non-zero.

GJ $= 25$ is he torsional stiffness of the material. Must be non-zero.

M $= 0.160$ is the mass per unit length of the material. Must be non-zero.

AM $= 0.05$ is the transverse added mass per unit length of the material.

WET $= 1.15$ is the wet weight.

D $= 0.009$ is the diameter of the material.

$C_{dt} = 0.01$ is the drag coefficient in the tangential (longitudinal) direction. Typical values for oceanographic cables range between 0.003 (for smooth cables) and 0.05 (for some faired cables).

$C_{dn} = 1.5$ is the drag coefficient in the normal (transverse) direction. Typically between 1.5 and 2.0 for standard circular oceanographic cables.

Similarly defined for others materials.

LAYOUT

TERMINAL = ANCHOR = CLUMP is the terminal definition, it must come both at the beginning and end of the list of segments and connectors.

SEGMENT = is a segment definition and consists of three required statements

- LENGTH = 2900 is the length of the segment.

- MATERIAL = WIRE is the material type to be used for this segment.

- NODES = (200,1.0) is the number and distribution of nodes to be used in discretizing the segment: (number of nodes, fraction of length), where the total number of nodes for the segment is derived from the number of nodes listed in each pair and the length fractions of all pairs must add to 1.0.

CONNECTOR = SHACKLE here specifies the optional connector that can be placed between segments. Omitting a connector between segments is one way to model a connection that does not transmit moments.

And so on until the other extreme oft he mooring: the buoy.

We don't report each step of the layout, but the essential to explain the logic of this last part of the input file.
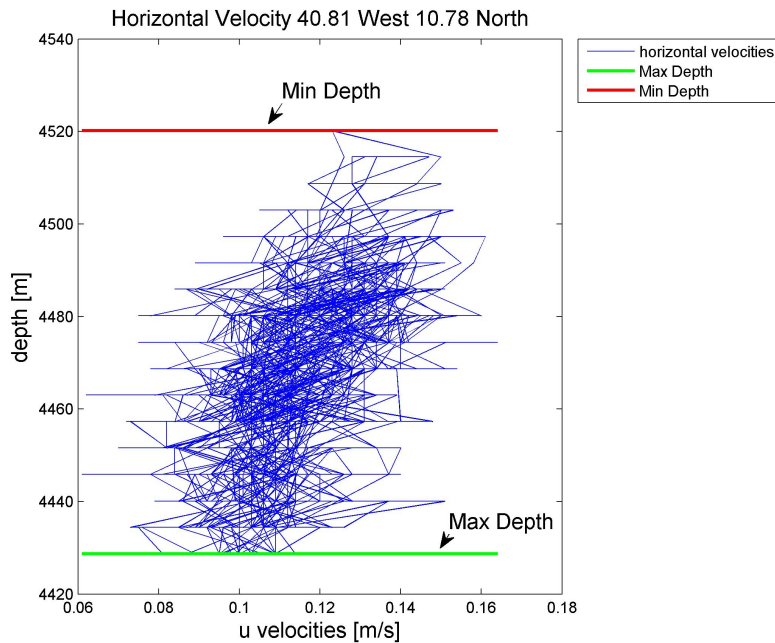
Figure 36: Horizontal velocities (x-axis) at the location 40 W 10 N. Notice that the measurements are made always in the vicinity of the same depth (y-axis), not along the water column. The minimum (4520.2 m) and maximum (4428.7 m) depths are also indicated

Animate

Cable through the Animate program window (see Fig. 37) can show us a movie of the design so far outlined . At the bottom of the window there are controls for creating plots and controlling the time rate of the animation. Along the right side are four toggle button/slider pairs which control the placement of marker nodes. The marker nodes are used to indicate which of the output nodes you want to view the results for. The toggle button under each slider activates one of the markers. Each marker is identified with a unique colour - this is the colour with which the time series or spectral results for that node will be drawn. The vertical black bars on each graph indicate the current time point. Which variables get plotted is controlled by the five buttons $\boxed{\text{D}}$ (displacements), $\boxed{\text{V}}$ (velocities), $\boxed{\text{F}}$ (forces), $\boxed{\text{M}}$ (moments), $\boxed{\text{E}}$ (Euler information). Each variable can be displayed as a function of time or of space, in global (earth-fixed) or local (Lagrangian) coordinates. Transformation between $\boxed{\text{total}}$ and dynamic only and local and $\boxed{\text{global}}$ coordinates can be made by clicking the appropriate button next to the plot controls. Spectra for time series results can be generated by clicking on the spectrum button at the bottom of the plot window (see Fig. 38).
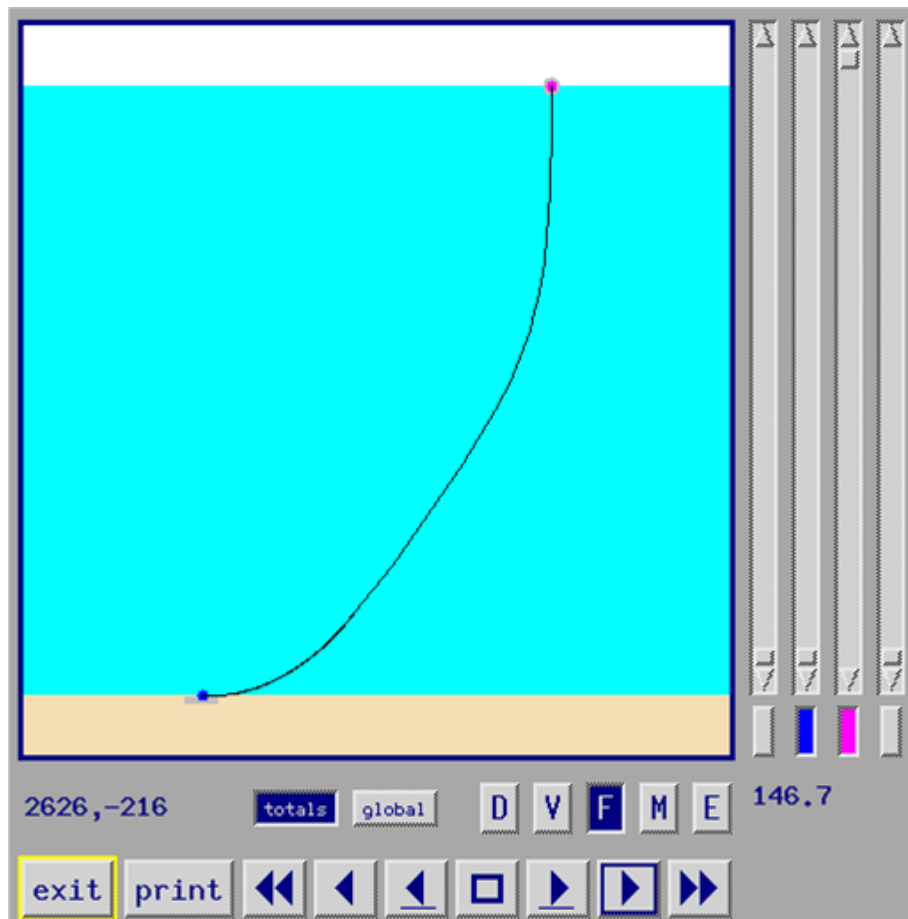
Figure 37: Animate window, showing the selected nodes (pink-buoy and blue-anchor) in which we want to display the magnitudes as a function of time. The magnitudes to display can be selected with the buttons $\boxed{D}$ (displacements), $\boxed{V}$ (velocities), $\boxed{F}$ (forces), $\boxed{M}$ (moments), $\boxed{E}$ (Euler information). We can also select the local/global ($\boxed{\text{global}}$) coordinates and the only dynamic/total ($\boxed{\text{total}}$) results.
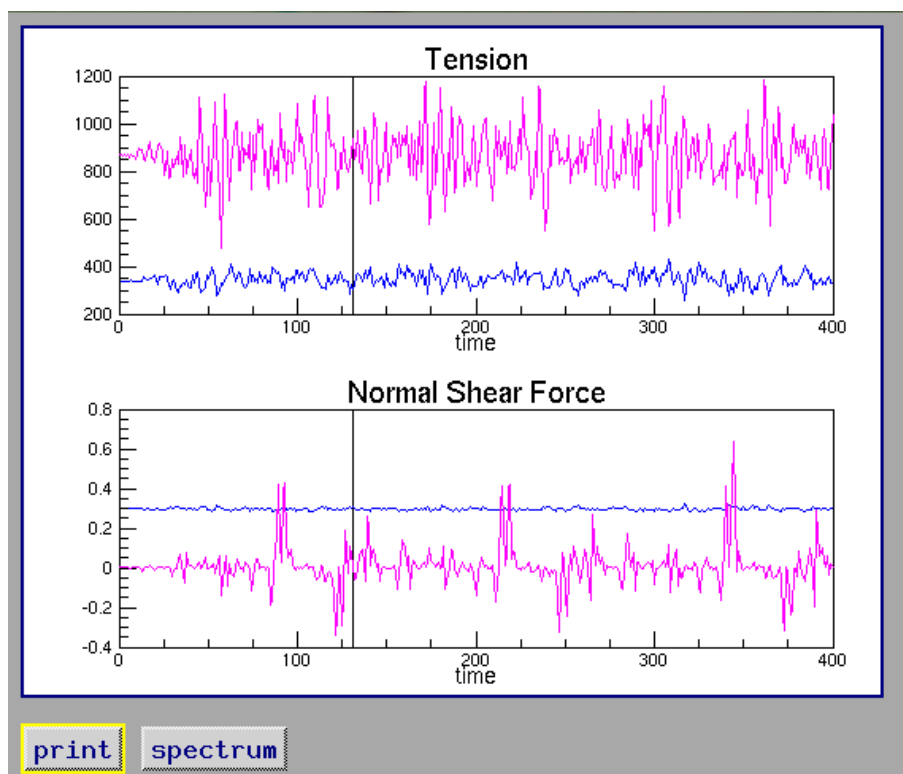
Figure 38: Time plot of the forces at marked nodes. The vertical black bars on each graph indicate the current time point. The colours indicates the two selected nodes (pink-buoy and blue-anchor).
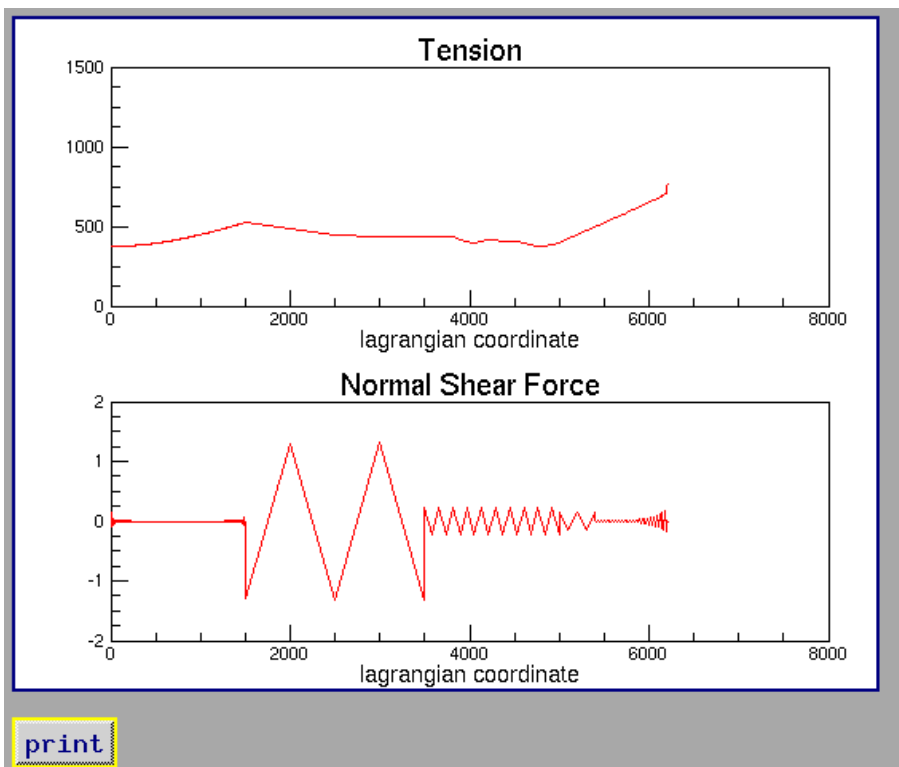
Figure 39: Snapshot of the forces along the mooring line. If the animation is playing then this graph keeps changing in time.
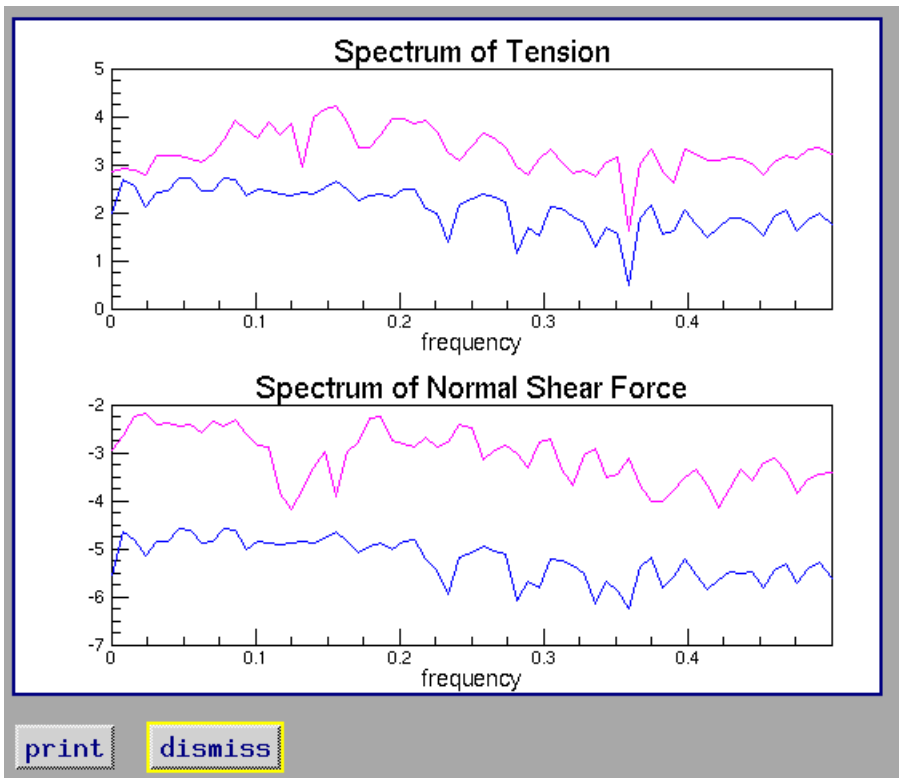
Figure 40: Spectra for time series tensions. The colours indicates the two selected nodes (pink-buoy and blue-anchor).

63

8   BVP Procedure

Bearing in mind what we said in Sec. 3.4, we have to imagine to put in the boundary described a floating body, on which we impose the impermeability condition (no flow through the border of the floating object).

Through a Fortran code, we can solve a 2D BVP to calculate the potential of velocity, the velocities, the pressure, the forces on the buoy and therefore, with the motion equation, its displacements.

The code can be used for three operational modes:

- radiation (for the heave motion we can imagine to push down the floating body and to observe it moving)

- small incoming wave and diffraction

- diffraction with the wave maker

To be able to write the motion equation we need to know which dynamic coefficients (added mass and damping) we have to apply. Using the radiation operational mode, it is possible to deduce these two coefficients, that according to Vugts [4] for a floating object depend on the oscillating frequency ω (therefore depend on the wave length according to the dispersion relation).

Setting the BVP for our case, we have to know that usually we use 10 segments for every wave length. At the same time we have to consider that maintaining the length of the segments we have to cover the entire depth of the water (5000 m). After some quick calculation we decide to use a wave length of 1000 m for which the results are reported in Fig. 41, where the x-axis represents the time and the y-axis the vertical force. The unexpected shape of the graph is due to the fact that around 20-25 seconds the reflected surface wave comes back toward the floating object.

This approach was important for this work to understand the physics of the problem. Even if there are already programs quite advanced in this field, their output, without knowing the theory, comes out of the blue and then it is difficult to fully exploit their potential.
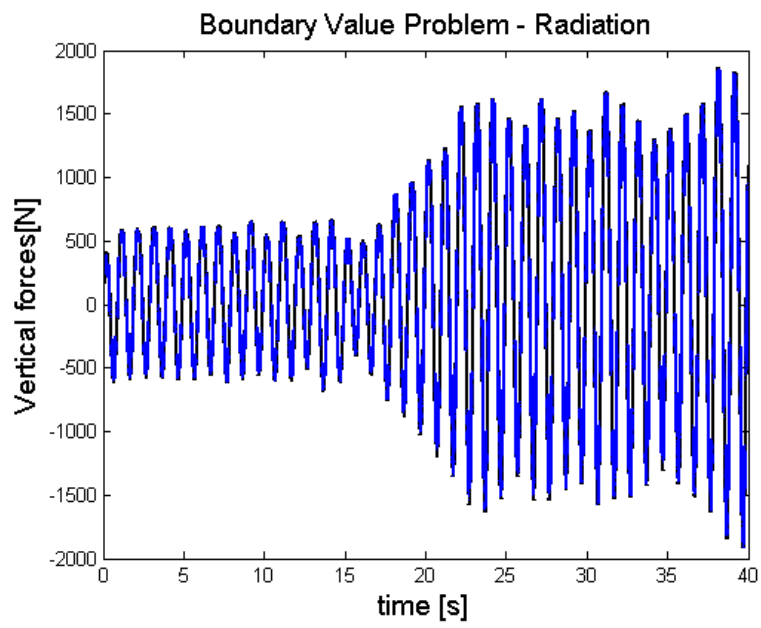
Figure 41: The x-axis represents the time and the y-axis the vertical force. The unexpected shape of the graph is due to the fact that around 20-25 seconds the reflected surface wave comes back towards the floating body.

9   Conclusions

So far it is possible to make some suggestions about the construction of a deep see surface mooring. Considering the environmental conditions and the requested instrument depths, the hybrid solution seems to be the best one. Due to the fact that the bottom part is made of wire it allows support of the deep instruments that we need. More over the middle part has an inverse catenary shape in slack current, so the buoy has a certain freedom to move following the shape of the surface waves without the mooring entering into resonance.

The MDD is important to become acquainted with the problem and maybe offers a preliminary design, but from the dynamic point of view is not helpful and, since the mooring has to face forces changing in time (surface waves forces, wind forces, currents, etc...) is important to study the behaviour of the floating buoy and of the mooring line in a certain window of time. For all these reasons a dynamic study is recommended. Even if *cable* is not user friendly and requires a deep knowledge of the element in line to built a database, it is a powerful tool to approach the design. Therefore it is strongly recommended. As shown in Fig. 42 a mooring that is not failing even in the worst situation according with a static approach maybe is failing dynamically.
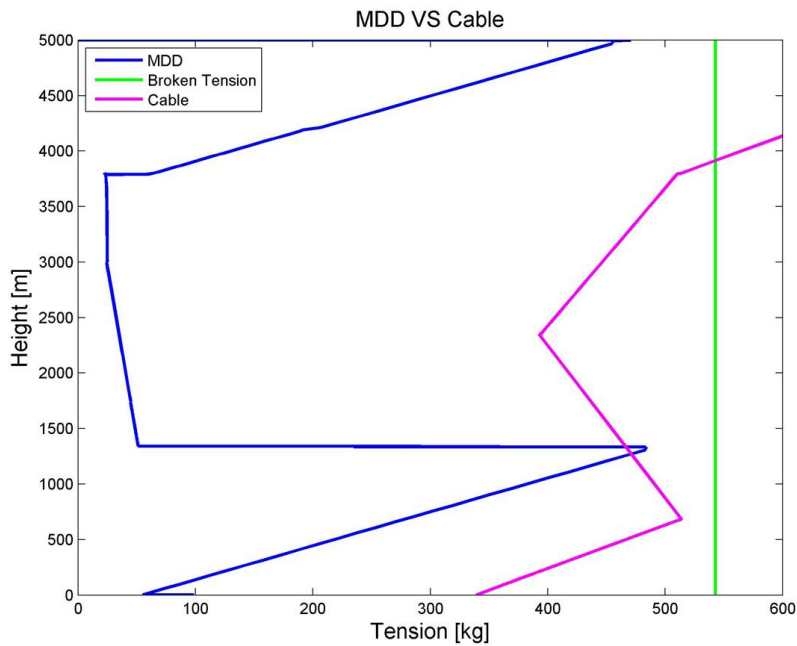
Figure 42: Comparison between tensions computed by MDD and tensions computed by *Cable* in worst case scenario and breaking tension. On the x-axis we can see the tension in Kg. On the y-axis we can see height of the mooring in the water. The green line represents the break tension of the wire. The blue the tensions along the line. The pink line shows the tensions computed by *Cable*.

Before changing the outlined design with MDD we need to dig deeper into the *cable* program to create a database suitable to our case. So for the moment

the preliminary design suggested is made of:

- 2700 m wire rope
- 1500 nylon
- 2000 polypropylene
- 3 in line buoys (two providing 250 kg of buoyancy and one 100)
- the Dolan floating buoy

10 Further Insight

For a first dynamic approach, as suggested by Grosenbaugh [3] (see Sec. 3.3), it could be useful to make a spectral analysis (see Fig. 43) of the movement of the mooring due to a certain sea state and comparing it with the spectrum of the amplitudes of waves to avoid resonant frequencies.
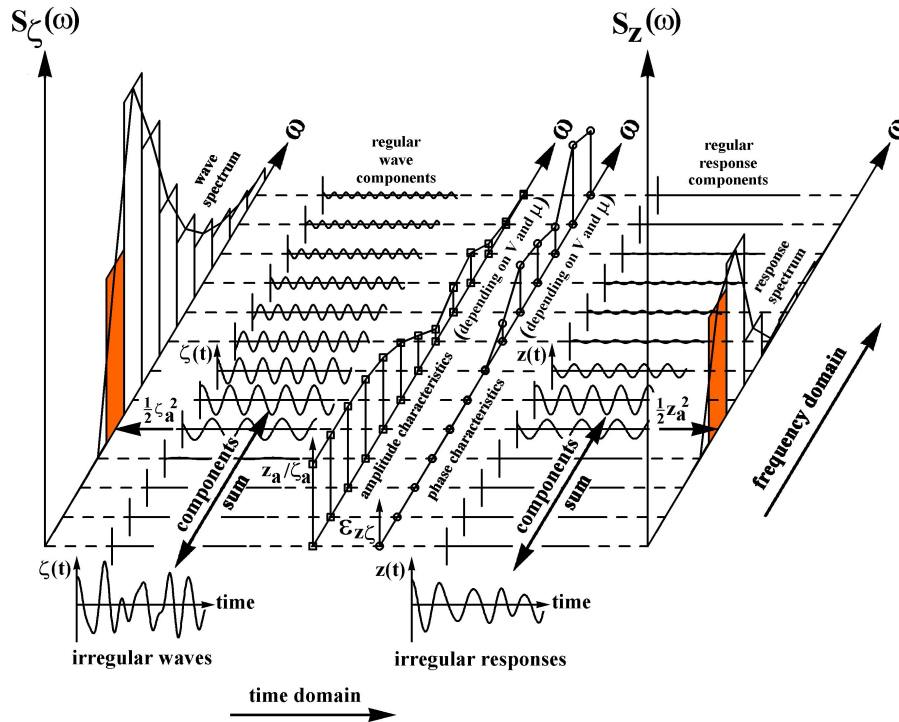
Figure 43: Here is represented a general spectrum of wave amplitudes along the ω axis. We can also see the representation in time of each harmonic component and, in foreground, there is the sum of all the components. [26]

Local resonance can also occur, the present solution to prevent this is that of shot peening the instruments as we saw in Sec. 3.1. With *cable* it is possible to observe the behaviour of a chosen point along the line and to make a spectral analysis, in this way a mechanical treatment, like the shot peening, can be avoided, especially on delicate instruments. Of course to do that we need to collect data on internal waves of the desired region.

Biofouling can also be a problem. Therefore to avoid the growth of organisms along the line in the euphotic zone, it is possible to use a cream generally used in farms with the animals (in Dutch "uierzalf"), which is not poisoning nor polluting.

It would be useful to proceed also with the understanding of the problem implementing the motion equation and comparing the output with the results coming from other programs.

The 3D analysis is definitely more suitable to this problem, especially during the study of the forces/displacements of the buoy. Studying a 2D floating body, for example, like in Sec. 3.4, can be useful for a large object, for which studying

just a "slice" of it can give results representative of all the other parts. But for a small body, like our buoy, just a "slice" of it is not enough to describe the geometry of most of the body and the forces on it (see Fig. 44). Therefore 3D effects become important.
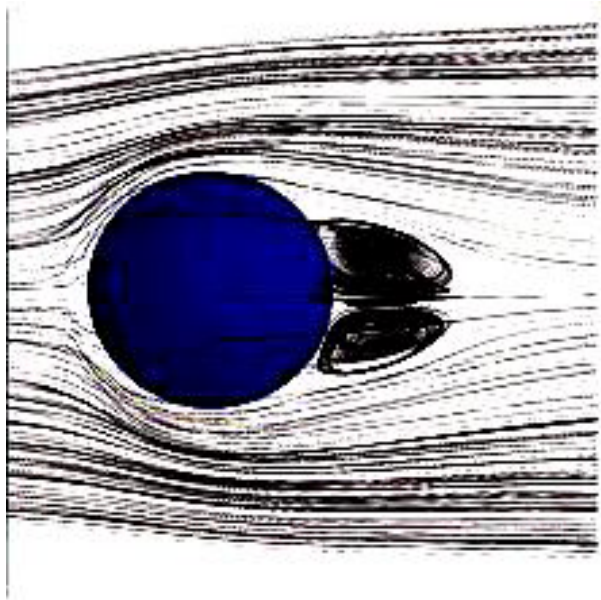
Figure 44: Illustration of the quick changing of the boundary layer, for which turbulent effects are present behind the blue sphere.

List of Figures

List of Tables

References

[1] R. K. Dewey. Mooring design & dynamics http://canuck.seos.uvic.ca/rkd/mooring/moordyn.php, May 2012.

[2] H.J.J. van den Boom. Dynamic Behaviour of Mooring Lines. *Behaviour of Offshore Structures, Elsevier Science Publishers B.V., Amsterdam*, pages 359–368, 1985.

[3] M. A. Grosenbaugh. On the dynamic of oceanographic surface moorings. *Ocean Engineering*, 23(1):7–25, 1994.

[4] G. Contento. *Lecture notes of Carichi Idrodinamici d′Onda*. Università degli studi di Trieste, 2011.

[5] Pan-European Infrastructure for Ocean and & Marine Data Management. http://seadatanet.maris2.nl/v_cdi_v2/search.asp, 2012.

[6] Marum Center for Marine Environmental Sciences. http://www.marum.de/en/index.html, May 2012.

[7] Marum Center for Marine Environmental Sciences. http://www.marum.de/binaries/binary13801/p1010183.jpg, May 2012.

[8] Marum Center for Marine Environmental Sciences. http://www.marum.de/binaries/binary13926/dscn5556.jpg, May 2012.

[9] Technicap. http://www.technicap.com/products/traps/pps6_2.htm, 2012.

[10] Woods Hole Oceanographic Institution WHOI. http://www.whoi.edu/, 2012.

[11] Southampton NOC, National Oceanography Centre. http://www.noc.soton.ac.uk/, 2012.

[12] National Institut of Ocean Technology NIOT. http://www.niot.res.in/, 2012.

[13] Fugro GEOS. http://www.geos.com/, 2012.

[14] French Research Institute for Exploration of the Sea Ifremer. http://wwz.ifremer.fr/institut_eng, 2012.

[15] Royal Netherlands Institute for Sea Research NIOZ. http://www.nioz.nl/, 2012.

[16] R.P.Trask and R.A.Weller. *Encyclopedia of Ocean Sciences,Moorings*, volume 3 (I-M).

[17] Web Design Metal Improvement Company. http://www.metalimprovement.com/company_overview.php, May 2012.

[18] M. Fujino T. Nakajima, S. Motora. On the dynamic analysis of multicomponent mooring lines. *OTC paper 4309*, 1982.

[19] K. Bathe and E.L Wilson. Numerical methods in finite element analysis. *International Journal for Numerical and Analytical Methods in Geomechanics*, 1976.

[20] K. Kokkinowrachos. Behaviour of vertical bodies of revolution in waves. *Ocean Engineering*, 13(6):505–538, 1986.

[21] R. Nabergoj. *Lecture notes of Teoria delle Onde*. 2010.

[22] G.F. Olliver N. Hogben, N.M.C. Dacunha. *Global Wave Statistics*. 1986.

[23] J.M.J. Journée and W.W. Massie. Offshore hydromechanics. *International Journal for Numerical and Analytical Methods in Geomechanics*, page 570, 2001.

[24] Wikipedia. http://en.wikipedia.org/wiki/ekman_spiral, May 2012 (The page was last modified on 10 April 2012 at 10:53.).

[25] J. I. Gobat and M. A. Grosenbaugh. *WHOI Cable v2.0: Time Domain Numerical Simulation of Moored and Towed Oceanographic Systems*. 2000.

[26] T. Sarpkaya and M. Isaacson. *Mechanics of Wave Forces on Offshore Structures*. 1981.

[27] R. K. Dewey. Mooring Design & Dynamics a Matlab package for designing and analyzing oceanographic moorings. *Marine Models*, pages 103–157, 1999.

Acknowledgements